20

ULTRASHORT OPTICAL SOURCES AND APPLICATIONS

Jean-Claude Diels

Departments of Physics and Electrical Engineering
University of New Mexico
Albuquerque, New Mexico

Ladan Arissian

Texas A&M University
College Station Texas, and
National Research Council of Canada
Ottawa, Ontario, Canada

20.1 INTRODUCTION

It is considered an easy task to control waveforms down to a few cycles with electronic circuits, at frequencies in the megahertz range. Ultrafast optics has seen the development of the same capability at optical frequencies, i.e., in the peta Hertz range. Laser pulses of a few optical cycles (pulse duration of a few femtoseconds) are routinely generated, with a suboptical cycle accuracy. The high power of these ultrashort bursts of electromagnetic radiation have led to new type of high field interactions. Electrons ejected from an atom/molecule by tunnel or multiphoton ionization can be recaptured by the next half optical cycle of opposite sign. The interaction of the returning electron with the atom/molecule is rich of new physics, including high harmonic generation, generation of single attosecond pulses of attosecond pulse trains, scattering of returning electrons by the atom/molecule, etc. Generation, amplification, control, and manipulation of optical pulses is an important starting point for these high field studies.

As compared to fast electronics, ultrafast optical pulses have reached a considerable higher level of accuracy. Pulse trains can be generated, of which the spacing between pulses (of the order of nanoseconds) is a measurable number of optical cycles (one optical cycle being approximately 2 fs in the visible). The frequency spectrum of these pulse trains is a frequency comb, of which each tooth can be an absolute standard with a subhertz accuracy. These frequency combs have numerous applications in metrology and physics—for instance, determining the eventual drift of physical constants, or in astronomy, a considerable improvement in the determination of Doppler shifts of various sources. In addition to the high level of accuracy and control in time and frequency, the femtoseconds sources have a remarkable amplitude stability. This stability is the result of nonlinear intracavity losses being minimum for a particular intensity.

This chapter starts with a detailed description of an optical pulse and an optical pulse train. Nonlinear mechanisms are described that can be exploited to control pulse duration, chirp, intensity

of the mode-locked lasers. In particular, a mode-locked laser with two intracavity pulses will be discussed, and its analogy with a quantum mechanical two-level system.

20.2 DESCRIPTION OF OPTICAL PULSES AND PULSE TRAINS

Single Optical Pulse

In this first section we will summarize the essential notations and definitions used throughout the chapter. Ideally, a mode-locked laser emits a continuous train of identical ultrashort pulses. To this infinite series of identical pulses corresponds, in the frequency domain, a finite (but large) number of equally spaced modes, generally referred to as a *frequency comb*. Inside the laser typically, only one pulse circulates. The shape of an intracavity pulse results from a steady-state equilibrium between various mechanisms of pulse stretching (saturable gain, dispersion), compression (saturable absorption, combination of self-phase modulation, and dispersion), amplification, and losses.

The pulse is characterized by measurable quantities which can be directly related to the electric field. A complex representation of the field amplitude is particularly convenient in dealing with propagation problems of electromagnetic pulses.

The complex spectrum of the pulse $\tilde{E}(\Omega)$* is defined by taking the complex Fourier transform $\mathcal{F}$ of the real electric field $E(t)=\varepsilon(t)\cos[\omega t+\varphi(t)]$:

$$\tilde{E}(\Omega)=\mathcal{F}\{E(t)\}=\int_{-\infty}^{\infty}E(t)e^{-i\Omega t}dt=\left|\tilde{E}(\Omega)\right|e^{i\Phi(\Omega)}=\tilde{\varepsilon}(\Omega-\omega)=\tilde{\varepsilon}(\Delta\Omega) \tag{1}$$

In the definition (1), $|\tilde{E}(\Omega)|$ denotes the spectral amplitude and $\Phi(\Omega)$ is the spectral phase Since $E(t)$ is a real function, its Fourier transform is symmetric, and its negative frequency part can be considered as redundant information. We will therefore choose to represent the light pulse by either the positive frequency function $\tilde{E}(\Omega)=E(\Omega)e^{i\Phi(\Omega)}$ (defined as being equal to zero for $\Omega<0$) or its complex inverse Fourier transform in the time domain

$$\tilde{E}(t)=\frac{1}{2\pi}\int_{0}^{\infty}\tilde{E}(\Omega)e^{i\Omega t}d\Omega=\frac{1}{2}\tilde{\varepsilon}(t)e^{i\omega t}=\frac{1}{2}\varepsilon(t)e^{i[\omega t+\varphi(t)]} \tag{2}$$

The relation with the real physical measurable field $E(t)$ is

$$E(t)=\tilde{E}(t)+\text{c.c.}=\varepsilon(t)\cos[\omega t+\varphi(t)] \tag{3}$$

The latter part of Eq. (2) defines a pulse envelope function $\varepsilon(t)$, a carrier frequency ω and a phase $\varphi(t)$. The decomposition is somewhat arbitrary, since the instantaneous frequency is given by

$$\omega(t)=\omega+\frac{4}{dt}\varphi(t) \tag{4}$$

In general, the carrier frequency ω will be chosen such that the average contribution from the phase factor $\varphi(t)$ is zero:

$$\langle\varphi(t)\rangle=\frac{\int_{-\infty}^{\infty}\varepsilon(t)^2\dot{\varphi}(t)dt}{\int_{-\infty}^{\infty}\varepsilon(t)^2dt}=0 \tag{5}$$

*Complex quantities related to the field will be represented with a tilde.

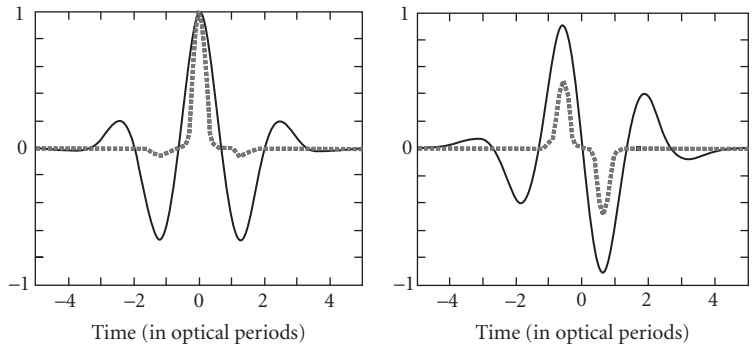

FIGURE 1 Comparison of a two-cycle pulse with $\varphi_e = 0$ (left) and $\varphi_e = \pi/2$ (right). The solid line traces the instantaneous electric field normalized to the peak value of its envelope, as a function of time in units of the optical period. The dotted lines correspond to the seventh power of the electric field, which would be driving a seven photon process.

For pulses of a few optical cycles, the variation of the phase factor can often be neglected across the pulse, and $\varphi(t) = \varphi_e$ is constant. Even for a single pulse, the phase factor φ_e is of practical significance, when a nonlinear phenomena traces the electric field under the envelope of a pulse of only a few cycle duration. If the phase φ_e is zero, the time dependence of the electric field is symmetric, with a peak in the center at $t = 0$, larger than the two opposite maxima at $t = \pm T/2$. If the phase $\varphi_e = \pi/2$, the time dependence of the electric field is antisymmetric, with equal opposite extrema at $t = \pm\pi/4$. These two pulses can give a different response in highly nonlinear phenomena. Let us consider for instance the shortest pulse that can be generated at 800 nm, which has a full width at half maximum (FWHM) of the intensity of 2.5 fs. Its complex electric field envelope can be written as $\tilde{\varepsilon}(t) = (\varepsilon_0/2)\exp[-(t/2T)^2 + i\varphi_e]$, which corresponds to the real electric field $E(t) = \varepsilon_0 \exp[-(t/2T)^2]\cos[2\pi(t/2T) + \varphi_e]$ which is plotted as a solid line in Fig. 1 for $\varphi_e = \pi/2$ (left) and $\varphi_e = \pi/2$ (right). If we consider that this pulse is used to excite a seven-photon process (for instance a seven-photon ionization), the driving function for that process is the seventh power of the field, which is plotted as a dotted line in Fig. 1. One can see that the different values of φ_e make a significant difference on how the process is driven. For $\varphi_e = 0$, the excitation is a single spike, as close approximation as practical to a δ-function. In the case of $\varphi_e = \pi/2$ (right), the excitation consists in a succession of positive and negative spikes.

Train of Pulses

The "ideal" mode-locked laser emits a train of identical pulses, at equal time interval. The period of the pulse train is τ_{RT}, defined as the separation between two successive envelopes. In the particular case that the pulse separation is an integer number of optical cycles $\tau_{RT} = NT = N/\nu$ (T being the light period and $\nu = \omega/(2\pi)$ the optical frequency) the successive pulses are identical. This will generally not be the case, and there will be a phase shift $\varphi_p = \omega\tau_{RT} \neq 2N\pi$ between successive pulses. The complex electric field of the total pulse train $\tilde{E}_{pt}$ is

$$\tilde{E}_{pt}(t) = e^{i\omega t}[\tilde{\varepsilon}(t) + \tilde{\varepsilon}(t - \tau_{RT})e^{i\varphi_p} + \tilde{\varepsilon}(t - 2\tau_{RT})e^{2i\varphi_p} + \cdots] \tag{6}$$

where $\tilde{\varepsilon}(t)=\varepsilon(t)e^{i\varphi_e}$ is the electric field of one particular pulse. The nth pulse has the phase factor $\exp[i(\varphi_e+n\varphi_p)]$, different from the previous and next pulse. To the change in phase between successive pulses φ_p, corresponds a frequency:

$$f_0=\frac{1}{2\pi}\frac{\varphi_p}{\tau_{RT}} \tag{7}$$

This frequency is called the *carrier to envelope offset.* The *carrier to envelope offset* is an important parameter of pulse trains, where the change in phase from pulse to pulse is a measurable quantity, independent of the duration of the individual pulse in the train.

One can "idealize" to the extreme the concept of a pulse train, by considering an infinite train of δ-functions, equally spaced by the period of the train τ_{RT}, as shown in Fig. 2*a*. The Fourier transform of this ideal pulse train shown in Fig. 2*b* is an identical picture in the frequency domain: a comb of infinite extent (because the pulses were δ-function in time), with δ-function teeth (because of the infinite extent of the train).

Since the comb extends to infinity, there is no particular tooth that can be called an average frequency. Each mode ν_m of index m carries the same weight, and corresponds in the time domain to an infinite sine wave, which is a particular term of a Fourier series representation of δ-function. The first tooth at frequency $\nu_0=f_0$ represents the carrier to envelope offset defined above. The corresponding carrier to envelope phase φ_e defined previously can be identified in the time domain, even with a train of δ-functions. The harmonic wave corresponding to the mode ν_2 is shown in Fig. 2*a*,* and the phase φ_e is identified as the phase at which each δ-function crosses the harmonic field. In the sketch of Fig. 2*a*, $\varphi_e=0$ for the first pulse, and φ_p is then the carrier to envelope phase φ_e of the second pulse as indicated in the figure.

A somewhat more mundane train of pulses of finite duration $\tau^\dagger$ is sketched in Fig. 3*a*. In the frequency domain (Fig. 3*b*), the infinite pulse train is represented by a finite frequency comb. The

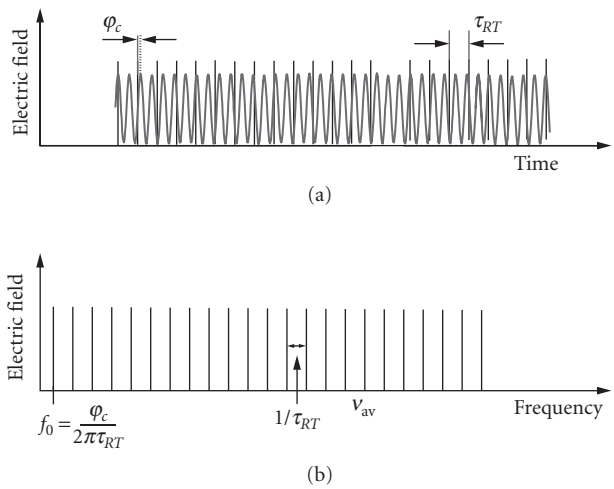

FIGURE 2 Idealized infinite train of δ-function pulses (*a*), and its Fourier transform (*b*). In (*a*), the carrier to envelope phase φ_e of the first pulse is assumed to be zero.

*This harmonic wave sketched is associated with ν_2 because there are two periods between pulses. In the Fourier spectrum of a train of δ-functions, any mode ν_n can be chosen as being the "average frequency".

†When not otherwise specified, the pulse duration will be the full width at half maximum (FWHM) of the pulse intensity profile.

ULTRASHORT OPTICAL SOURCES AND APPLICATIONS

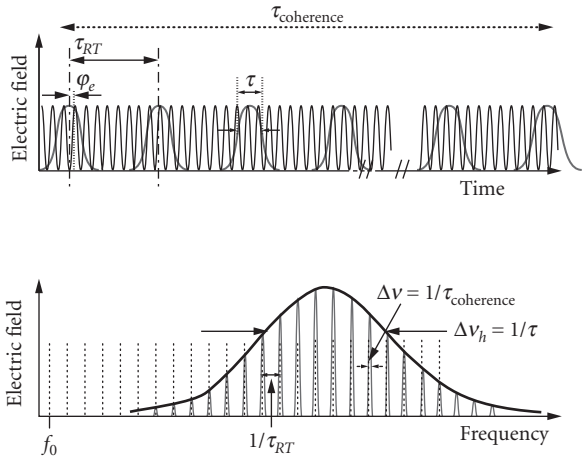

FIGURE 3 (*a*) Train of pulses of finite duration τ. The successive pulse envelope repeats every τ_{RT}. Within the coherence time of the train $T_{coherence}$, it is the same carrier at the optical frequency that is modulated by the successive envelopes. (*b*) The Fourier transform of the pulse train shown in (*a*).

envelope of the comb is the Fourier transform of the envelope of a single pulse of the train, thus of extension $\approx 1/\tau$. The teeth of the frequency comb are no longer δ-functions, but sharp peaks of width $1/\tau_c$, where τ_c is the coherence time of the pulse train. The carrier to envelope phase φ_p is indicated for a pulse of the time sequence in Fig. 3*a*. Note that this phase is changing from one pulse to the next. The rate of change $\varphi_p/(2\pi\tau_{RT})$ is the frequency f_0, which is indicated in the frequency picture by the lowest frequency tooth of the extension (dashed lines in Fig. 3*b*).

The angular frequency ω_m of the mth mode of the comb is given by

$$\omega_m = 2\pi f_0 + m\frac{2\pi}{\tau_{RT}} \tag{8}$$

In the case of a train of pulses of finite duration, the frequency f_0 is no longer a real tooth of the comb, but the first mode of an extension of the frequency comb beyond the pulse bandwidth as shown by the dotted line in (Fig. 3*b*).

It can be seen from this definition that f_0 is indeed the change of phase per round-trip between the envelope and the carrier. By definition of τ_{RT}, the pulse envelope peaks exactly at the same locations after one round-trip. With respect to this envelope, the shift of phase of the mode m is obtained by multiplying Eq. (8) by τ_{RT}:

$$\omega_m \tau_{RT} = 2\pi f_0 \tau_{RT} + 2m\pi \tag{9}$$

which, after substitution of the definition of f_0 Eq. (7), is indeed the phase φ_p defined earlier.

Soliton Solution and Steady-State Pulse Train

As mentioned in the introduction, if a laser is to generate a pulse of well defined duration and shape, there has to be compression and broadening mechanisms that balance each other, and lead to

a stable pulse. The mechanisms that lead to an emergence of a pulse out of noise in a laser cavity are usually dissipative, i.e., the pulse that emerges dissipates a minimum amount of energy by nonlinear loss mechanisms and extracts the maximum amount of gain from the active laser medium. We will consider in this section only nondissipative interaction that plays a dominant role for the stable formation of the shortest pulses. First we consider the evolution of a single pulse as it propagates through a cavity. Next we will study the formation of a pulse train with a similar nondissipative model.

Evolution of a Single Pulse in an "Ideal" Cavity When a laser is in continuous operation, the cavity gain and losses are in equilibrium. In the case of femtosecond mode-locked lasers, the major pulse-shaping mechanism is a combination of self-phase modulation and dispersion at each round-trip. The self-phase modulation results from a nonlinear index of refraction $n_2 I$ (I being the intensity in W/cm^2, n_2 being the nonlinear index in cm^2/W of a nonlinear element of length ℓ in the cavity). The dispersion k'' results from the frequency dependence of the average index of refraction n_{av} defined previously, and is characterized by the second derivative of a cavity averaged k vector with respect to frequency. In what follows, for simplicity, we will neglect higher-order terms in Kerr effect and in dispersion. The evolution of a pulse in the mode-locked laser cavity can be considered as a propagation (of a nondiffracting beam) through an infinite lossless medium, with a positive Kerr nonlinearity ($n_2 > 0$) and a negative dispersion (as can be introduced with intracavity prisms[1] or chirped mirrors[2] in the cavity). The pulse evolution generally converges toward a steady-state solution, designated as "solitons," which can be explained as follows. The nonlinearity is responsible for spectral broadening and up-chirp. Because of the anomalous dispersion, $k'' < 0$, the high-frequency components produced in the trailing part of the pulse, travel faster than the low-frequency components of the pulse leading edge. Therefore, the tendency of pulse broadening owing to the exclusive action of group velocity dispersion can be counterbalanced. To determine the approximate parameters of that solution, let us assume a Gaussian pulse $\varepsilon(t) = \varepsilon_0 \exp[-(t/\tau_{G0})^2]$, and let us state that the chirp produced in the pulse center by the nonlinearity and the dispersion are of equal magnitude (but of opposite sign). Under this equilibrium condition the pulse circulates in the cavity without developing a frequency modulation and spectral broadening. The effect of group velocity dispersion is to create a pulse broadening and a down-chirp (in a medium of negative dispersion). The change (per round-trip) of the second derivative of the phase versus time, at the center of the pulse, is given, in a first-order approximation, by Ref. 3:

$$\Delta\left(\left.\frac{\partial^2 \varphi(t)}{\partial t^2}\right|_{(t=0)}\right) = \frac{4k''_{av}}{\tau_{G0}^4} P \tag{10}$$

where $k''_{av} = d^2 k_{av}/d\Omega^2$ is the second-order dispersion averaged over the cavity of perimeter P, which is < 0 for an optical element with negative dispersion. Assuming that the cavity contains an element with a nonlinear index $n = n_0 + n_2 I$ of length ℓ_{Kerr}, the phase induced by self-phase modulation, near the center of the Gaussian pulse, is

$$\Delta\varphi(t) = -k_{NL} \cdot \ell_{Kerr}\Big|_{(t=0)} = \frac{2\pi n_2}{\lambda} \ell_{Kerr} I \approx \frac{4\pi n_2 I_0 \ell_{Kerr}}{\lambda} \frac{t}{\tau_{G0}^2} \tag{11}$$

where we have used a quadratic approximation for the Gaussian near $t = 0$. Taking the second derivative yields the chirp induced by phase modulation at the pulse center:

$$\Delta\left(\frac{\partial^2 \varphi(t)}{\partial t^2}\right) \approx \frac{8\pi n_2 I_0 \ell_{Kerr}}{\lambda \tau_{G0}^2} \tag{12}$$

ULTRASHORT OPTICAL SOURCES AND APPLICATIONS

The peak intensity of the pulse (at $t = 0$) is $I_0 = \varepsilon_0^2/2\eta$; $\eta = \sqrt{\mu_0/\epsilon}$ being the characteristic impedance of the medium. Expressing that the chirps induced by phase modulation [Eq. (12)] and dispersion [Eq. (10)] should cancel each other leads to

$$I_0 \tau_{G0}^2 = -\frac{\lambda k''_{\text{av}}}{2\pi n_2} \frac{P}{\ell_{\text{Kerr}}} \tag{13}$$

This expression leads to a value for the pulse duration given by

$$\tau_{G0}^2 = \frac{\lambda |k''_{\text{av}}|}{2\pi n_2 I_0} \frac{P}{\ell_{\text{Kerr}}} \tag{14}$$

In a Ti:sapphire laser, $n_2 = 10.5 \cdot 10^{16}$ cm^2/W; the crystal length is typically $\ell = 4$ mm, and a well-designed laser can produce a train of 10 fs pulses with an intracavity average power of the order of 10 W. These numbers can be used in Eq. (14) to determine the negative cavity dispersion k''_{av} required for stable laser operation.

How Unequally Spaced Modes Lead to a Perfect Frequency Comb The physical reason for a non-zero carrier to envelope offset f_0 is the dispersion of the laser cavity in which a pulse is circulating. The components of the laser cavity impose different group velocities on the pulse. We can define an average group velocity $v_g = P/\tau_{RT}$ of the pulse envelope, where P represents twice the length of a linear cavity, or the perimeter of a ring cavity. That group velocity is different from the phase velocity c/n_{av} (n_{av} being the linear index of refraction averaged over the laser components). The two quantities are related by

$$\frac{1}{v_g} = \frac{n_{\text{av}}}{c} + \frac{\omega}{c} \frac{dn_{\text{av}}}{d\Omega}\bigg|_{\omega} \tag{15}$$

Note that these quantities n_{av} and v_g are function of the spectral frequency of the pulse. The "ideal mode-locked laser" considered in this section already poses a conceptual dilemma. Mode-locking is generally described as putting the modes of a laser cavity in phase. If the cavity has dispersion, we have seen that the mode-comb issued from the laser does not start at zero frequency but with a frequency offset f_0. Keeping in mind that a cavity with dispersion has unequally spaced modes, is contradictory to the fact that the frequency comb has rigourously equally spaced teeth.* To resolve this apparent contradiction, we will look at the pulse train formation, and discuss how an initially irregular set of modes can lead to a perfect frequency comb.

As shown above, a minimum negative cavity dispersion k''_{av} is required for stable mode-locked operation. Such a cavity dispersion implies that the index of refraction n_{av} is frequency (wavelength) dependent, hence the spacing of the cavity modes $c/[n_{\text{av}}(\Omega)P]$ varies across the pulse spectrum.

The laser is modeled by a circulating pulse, which enters a Kerr medium of thickness ℓ, resulting in phase modulation at each passage, and a medium that represents the linear dispersive properties of the cavity. We will assume that the balance of gain and losses maintains a constant Gaussian shape for the envelope of the circulating pulse. At each passage through the cavity, the phase of the pulse is modified in the time domain through the Kerr effect, and in the frequency domain through dispersion. We consider first the modulation in the time domain:

$$\varphi(t) = -k_{NL} \ell_{\text{Kerr}} = -\frac{2\pi n_2 \ell_{\text{Kerr}}}{\lambda} I_0 e^{-2(t/\tau_G)^2} \tag{16}$$

*A fact that has been verified experimentally with millihertz accuracy.[4]

where τ_G is the $1/e$ half-width of the pulse electric field envelope (the FWHM of the intensity is $\tau_p = \sqrt{2\ln 2}\tau_G$). Ignoring at this point the influence of dispersion (which will be introduced after Fourier transformation into the frequency domain), the pulse *train* issued from the laser can be represented by

$$\sum_{q=0}^{\infty} \varepsilon(t-\tau_q) e^{iq\varphi(t-\tau_q)} e^{i\omega t} \tag{17}$$

where τ_q is the time of arrival of the center of gravity of the successive pulses. At this point τ_q is not set to any value. It is assumed here that at $t = 0$, the first pulse is unmodulated. Using a parabolic approximation for the Gaussian intensity profile, the time-dependent phase is

$$\varphi(t-\tau_q) \approx \frac{4\pi n_2 I_0 \ell_{\text{Kerr}}}{\lambda}\left(\frac{t-\tau_q}{\tau_G}\right)^2 = a\left(\frac{t-\tau_q}{\tau_G}\right)^2 \tag{18}$$

The Fourier transform of the pulse train given by Eq. (17) is

$$\varepsilon(\Delta\Omega)\left[\sum_{q=0}^{\infty} e^{i\Delta\Omega\tau_q} e^{iq\Delta\Omega^2\tau_k^2}\right] \tag{19}$$

where

$$\begin{aligned} \Delta\Omega &= \Omega - \omega \\ \varepsilon(\Delta\Omega) &= \frac{\varepsilon_0\sqrt{\pi}\tau_G}{\sqrt[4]{1+a^2}} \exp\left\{-\frac{\Delta\Omega^2\tau_G^2}{4(1+a^2)}\right\} \\ \tau_k^2 &= \frac{a\tau_G^2}{4(1+a^2)} \end{aligned} \tag{20}$$

The width of the Gaussian pulse spectrum, broadened by the Kerr effect, is the inverse of the characteristic time τ_k. Let us now take dispersion into account. The operation representing the dispersion of the cavity is a product of the spectral field by $\exp[-ik_{\text{av}}(\Delta\Omega)P]$, where $-k_{\text{av}}(\Delta\Omega)P^*$ is the phase change per round-trip. The combined Kerr effect and dispersion, in the frequency domain, leads to the output spectral field:

$$\varepsilon_{\text{out}}(\Delta\Omega) = \varepsilon(\Delta\Omega)\left[\sum_{q=0}^{\infty} e^{i\Delta\Omega\tau_q} e^{iq\Delta\Omega^2\tau_k^2} e^{-iqk_{\text{av}}(\Delta\Omega)P}\right] \tag{21}$$

Expanding the wave vector $k_{\text{av}}(\Delta\Omega)$ in series, to second order:

$$\begin{aligned} k_{\text{av}}(\Delta\Omega)P &= k_{\text{av}}(\Delta\Omega=0)P + \Delta\Omega k'_{\text{av}}P + \frac{\Delta\Omega^2}{2}k''_{\text{av}}P \\ &= k_{\text{av}}(\Delta\Omega=0)P + \Delta\Omega\tau_{RT} + \frac{k''_{\text{av}}P}{2}\Delta\Omega^2 \end{aligned} \tag{22}$$

*In the argument of k_{av}, the light frequency ω is taken as origin ($\Delta\Omega = 0$) of the frequency scale.

where the derivatives k'_{av} and k''_{av} are calculated at the light frequency $\omega(\Delta\Omega=0)$. Note that $k'_{av}=1/v_g=\tau_{RT}/P$ [cf. Eq. (15)] are material properties independent of the index q, as is the cavity perimeter P. The modes of the cavity are not equally spaced. The parameter k'' characterizes the departure from equal spacing. Substituting (22) in Eq. (21),

$$\mathcal{E}_{out}(\Delta\Omega)=\mathcal{E}(\Delta\Omega)\left[\sum_{q=0}^{\infty}e^{i\Delta\Omega(\tau_q-q\tau_{RT})}e^{iq\Delta\Omega^2(\tau_k^2-k''_{av}P/2)}\right] \tag{23}$$

The conditions

$$\tau_k^2=-\frac{k''_{av}P}{2} \tag{24}$$

$$\tau_q=(q+1)\tau_{RT} \tag{25}$$

leads to modes that are exactly equally spaced. The inverse Fourier transform of the frequency comb becomes then

$$\tilde{\mathcal{E}}_{out}(t)=\mathcal{E}(t)+\mathcal{E}(t-\tau_{RT})e^{-ik_{av0}P}+\mathcal{E}(t-2\tau_{RT})e^{-2k_{av0}P}+\cdots \tag{26}$$

This last equation corresponds indeed to the description of the ideal frequency comb, with equally spaced pulses in time and frequency, and a carrier to envelope phase shift of $\varphi_p=-k_{av0}P$. In the case of small Kerr modulation, $a\ll 1$, it can easily be verified that the condition in Eq. (24) is identical to the soliton Eq. (14). Indeed, substituting

$$\tau_k^2=\frac{a\tau_G^2}{4(1+a^2)}\approx\frac{4\pi n_2 I_0 \ell_{Kerr}\tau_G^2}{4\lambda}=\frac{k''_{av}P}{2} \tag{27}$$

which is indeed equivalent to Eq. (14). One can thus conclude that the mechanism that leads to an equal spacing for the teeth of the frequency comb emitted by the laser is the same Kerr effect responsible for creating maximum intracavity pulse compression.

20.3 PULSE EVOLUTION TOWARD STEADY STATE

A Simple Model

In the previous section we have considered the dispersive mechanisms that ultimately give the final shape in amplitude and phase to the steady-state pulse. This mechanism dominates in the subpicosecond regime, where dissipative mechanism have reached equilibrium. Other elements play a decisive role in initiating the mode-locking, which are usually referred to as the passive mode-locking elements. The latter can most often be represented by intensity-dependent intracavity loss. Larger losses at low intensity imply that the laser has less gain—and may be below threshold—for low-intensity continuous wave (cw) radiation than for pulses with higher peak intensity. This leads to the emergence of a pulse out of the amplified spontaneous emission noise of the laser. Rather than concentrating on the primary process of formation of a precursor of a pulse from random noise, let us follow the evolution of the pulse from its birth from noise until it has blossomed into a fully shaped stable laser pulse. In this intermediate stage of the evolution toward steady state, the main shaping elements are dissipative, as opposed to the purely dispersive interaction considered in the previous section. We will look for simple evolution equations for the pulse energy $W=\int_{-\infty}^{\infty}I(t)dt$, with $I(t)$ being the pulse intensity. The element responsible for saturable losses (gain) should have

typically a *linear* loss (gain) factor at low energies, and a *constant* loss (gain) at higher energies. We thus have, at low energies: $dW/dz = \mp\alpha W$. At large energies $W \gg W_s$: $dW/dz = \mp W_s$ where W_s is the saturation energy for the chosen geometry. The simplest differential equation to combine these two limits is

$$\frac{dW}{dz} = \alpha_g W_{sg}\left[1 - e^{W/W_{sg}}\right] \tag{28}$$

Equation (28) is written for a medium with a linear gain α_g and a saturation energy W_{sg}. It can be integrated to yield the energy W_2 at the end of the amplifier of thickness d_g, as a function of the input energy W_1:

$$W_2 = G(W_2, W_1)W_1 = W_{sg} \ln\left\{1 - e^{\alpha_g d_g}(1 - e^{W_1/W_{sg}})\right\} \tag{29}$$

A similar equation applies to the saturable absorber, with a negative absorption coefficient $-\alpha_a$ and a smaller saturation energy W_{sa}:

$$W_2 = A(W_2, W_1)W_1 = W_{sa} \ln\left\{1 - e^{\alpha_a d_a}(1 - e^{W_1/W_{sa}})\right\} \tag{30}$$

The dominant linear loss element is the output coupler, with (intensity) reflectivity r. The transfer function for that element is simply

$$W_2 = L(W_2, W_1)W_1 = rW_1 \tag{31}$$

and the energy of the output pulse is $(1-r)W_1$. The evolution of the pulse energy in a single round-trip can be simply calculated from the product of all three transfer functions given by Eqs. (29), (30), and (31). For instance, if we consider a ring laser with the sequence: mirror, gain, and absorber, the pulse energy W_4 after the absorber is given by the product $A(W_4, W_3)G(W_3, W_2)L(W_2, W_1)$. One can also express the relation between the energy W_4 and the pulse energy W_1 before the output mirror by the algebraic relation:

$$1 + a[e^{W_4/W_{sa}} - 1] = \left\{1 + g[e^{rW_1/W_{sg}} - 1]\right\}^{W_{sg}/W_{sa}} \tag{32}$$

where $a = \exp\{-\alpha_a d_a\}$ is the *linear* small-signal attenuation of the passive element and $g = \exp\{\alpha_g d_g\}$ is the *linear* small-signal amplification.

High-Gain Oscillators

Unlike laser amplifiers, where it is desirable to use a gain medium with as high a saturation energy density as possible, mode-locked oscillators will often use high-gain laser media. These are opposite requirements: the larger the amplification cross section σ_g, the larger the gain $\alpha_g = \Delta N \sigma_g$, and the smaller the saturation energy density $W_s = \hbar\omega/(2\sigma_g)$. Both numbers a and g can be large, and the reflectivity of the output coupler r can be even lower than 50 percent. Examples are dye lasers, semiconductor lasers with tapered amplifiers, and to a smaller extend the T:sapphire laser. As a result, the order of the elements matters in the design of the laser, and in its performances. To illustrate this point, let us assume that the passive element is totally saturated in normal operation. In full saturation, the input energy $W(0)$ is related to the output energy $W(d)$ by

$$W(d) = W(0) - \alpha_a d_a W_{sa} \tag{33}$$

Given an initial energy W_1, the energy W_4 for a single passage through three different sequences of the same elements is given below. For the sequence mirror-absorber-gain

$$e^{W_4/W_{sg}} = 1 - g\left[1 - e^{(rW_1 - \alpha_a d_a W_{sa})/W_{sg}}\right] \tag{34}$$

For the sequence absorber-mirror-gain

$$e^{W_4/W_{sg}} = 1 - g\left[1 - e^{r(W_1 - \alpha_a d_a W_{sa})/W_{sg}}\right] \tag{35}$$

For the sequence absorber-gain-mirror

$$e^{W_4/W_{sg}} = \left\{1 - g\left[1 - e^{(W_1 - \alpha_a d_a W_{sa})/W_{sg}}\right]\right\}^{1/r} \tag{36}$$

Let us take a numerical example for a high-gain system such as the flash-lamp pumped Nd: glass laser, with $W_{sa}/W_{sg} = 0.1$, $\alpha_a d_a = 1$, $\alpha_g d_g = 1.5$ and output coupling of $r = 0.5$. For an initial energy $W_1/W_{sg} = 0.5$, we find for the sequence absorber-mirror-gain $W_4/W_{sg} = 0.689$, and for the sequence absorber-gain-mirror $W_4/W_{sg} = 0.582$. The order of the elements, the relative saturation of the gain to that of the passive element, as well as the output coupling influence the stability and output power of the laser, as shown in Ref. 5. The evolution of the pulse in the cavity can be calculated by repeated applications of products of operations such as $A(W_4, W_3)G(W_3, W_2)L(W_2, W_1)$ for the sequence (passive element, gain, output coupler), starting from a minimum value of W_1 above threshold for pulsed operation, and recycling at each step the value of W_4 as the new input energy W_1. Figure 4 shows the growth of intracavity pulse energy as a function of the round-trip index j, for different orders of the elements. The initial pulse energy is 1 percent of the saturation energy W_{sg} in the gain medium. The saturation energy and optical thickness of the absorbing medium are, respectively, $W_{sa} = 0.8W_{sg}$ and $\alpha_a d_a = 1.2$. The linear gain is $\alpha_g d_g = 1.5$ and the output coupling $r = 0.8$.

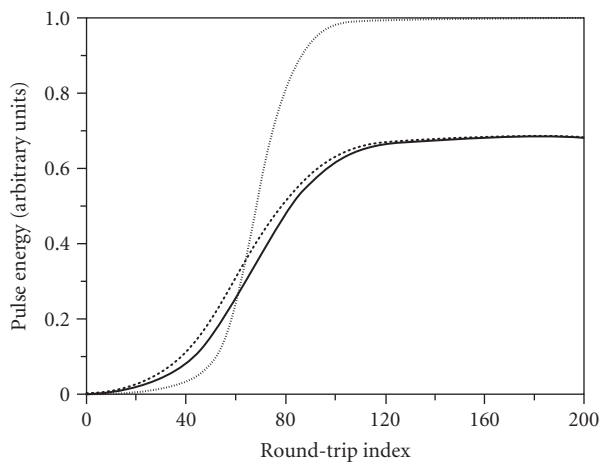

FIGURE 4 Intracavity pulse energy versus round-trip index j. The solid, dashed, and dotted lines correspond to the sequence m(irror)–a(bsorber)–g(ain), a–g–m and a–m–g, respectively.

The main point of this exercise is that the order of the elements is important, a fact confirmed by measurement on moderate-gain lasers such as Ti:Al_2O_3. Such dependence on the order of the elements indicates that analytical theories based on the approximation of infinitesimal change per element and per cavity round-trip are not quite adequate. Numerical codes have been developed that attempt to include all physical phenomena affecting pulse shape and duration. Unfortunately, the shear number of these mechanisms makes it difficult to reach a physical understanding of the pulse-generation process, or even identify the essential parameters. Therefore, the most popular approach is to construct a simplified analytical model on a selected mechanism.

20.4 COUPLING CIRCULATING PULSES INSIDE A CAVITY

Pulse Train Interferometry

A pulse train combines the temporal resolution of a single pulse, and the spectral resolution of a cw beam. It is therefore not surprising that new interferometric technique can be developed exploiting these properties.

Because the ratio of pulse duration to the period of the train is generally less than $1:10^5$, interferences of pulse trains of different repetition rates will not be considered here. We will instead focus on a situation where two pulse trains of identical repetition rate, but different carrier to envelope phase, are made to interfere. It will be shown in the next section how pulse trains of identical repetition rate are generated. The experimental arrangement for pulse train interferometry is depicted in Fig. 5. The two pulse trains are combined by a beam splitter, and their relative delay adjusted in an optical delay line, in order to have superposition of the pulse envelopes on the detector. If the carrier to envelope phase is identical for both pulse trains, the detector will simply register a constant signal, with an amplitude dependent on the relative phase of the two trains at the detector.

If instead the two pulse trains have a different carrier to envelope phase, successive pulses will interfere differently. The envelope of the interfering pulse trains, as seen by the detector, will be modulated at the frequency $f_{01} - f_{02}$, where f_{01} and f_{02} are the carrier to envelope offsets of either pulse trains.

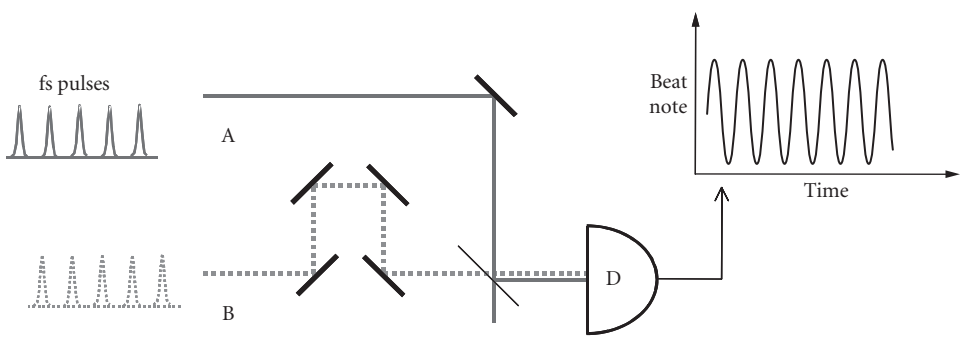

FIGURE 5 Interference of two pulse trains of the same repetition rate. An optical delay line is required to ensure temporal overlap of the pulses in either train.

Interwoven Pulse Trains Generated by Two Intracavity Pulses

We have seen the interference of pulse trains. These can be generated by a laser cavity. Inside the laser, there are then two or more pulses circulating in the cavity. The interactions of these two pulses will determine the relative properties of the pulse trains. The common picture of the mode locked laser is that of a resonator cavity with gain in which a single pulse circulates. It is interesting to consider, both from the point of view of fundamental understanding of the laser operation and applications to sensors, the situation where several pulses circulate in the cavity. Mode-locking with multiple pulses/round-trip is sometimes referred to as "harmonic mode-locking" 6–10. Techniques of harmonic mode-locking have been developed for telecommunications, where a pulse rate of over a GHz is desirable. The fundamental clock remains the round-trip time, which may typically be of the order of 100 MHz. If there are m pulses in the cavity, there will be m values of interpulse delay, which, in the frequency domain, will mean some splitting of the modes, which, is small, may be seen as a slight broadening of the tooth of the comb.

In the following we will consider only the case of two pulses circulating in the cavity, separated exactly by half the cavity round-tip time. Such a situation is encountered in bidirectional ring lasers, but also in linear cavities. Of particular interest is to determine the type of coupling that may or may not exist between the two pulses, and the resulting correlation between the two pulse trains. As will be the case in most sensor applications,[11] we will assume in the following that the two pulses experience a relative shift in phase δ at each round-trip.

Locking Two Pulse Trains by Backscattering

Whether in a ring or linear laser, the two circulating pulses will meet at two points of the cavity. Unless the meeting point is in vacuum, there will be some coupling introduced by the medium in which the pulses meet. The most common case is that of a medium with random scattering. Using the plane wave description of Eq. (2), the backscattering component $\tilde{r}_{ij} = r\exp(\theta_{ij})$ of scattering will couple the pulse with field envelope $\tilde{\varepsilon}_j$ into the pulse with field envelope $\tilde{\varepsilon}_i$:

$$\begin{aligned}\frac{\partial\tilde{\varepsilon}_1}{\partial t} &= i\frac{\delta}{2\tau_{RT}}\tilde{\varepsilon}_1 + \frac{1}{\tau_{RT}}\tilde{r}_{12}\tilde{\varepsilon}_2 \\ \frac{\partial\tilde{\varepsilon}_2}{\partial t} &= \frac{1}{\tau_{RT}}\tilde{r}_{21}\tilde{\varepsilon}_1 - i\frac{\delta}{2\tau_{RT}}\tilde{\varepsilon}_2\end{aligned} \tag{37}$$

Of particular interest here is the impact of the coupling on the phase of the two fields, since the balance of saturable gain and losses will in general restore a steady-state value of the pulses energy. Expressing the fields in terms of amplitude and phase as in Eq. (2) in the system of Eqs. (37), and taking the difference of the imaginary parts, yields:

$$\frac{\partial(\varphi_2-\varphi_1)}{\partial t} = \frac{\partial\psi}{\partial t} = \frac{\delta}{\tau_{RT}} + \frac{r}{\varepsilon_1\varepsilon_2\tau_{RT}}[\varepsilon_1^2\sin(\theta_{21}-\psi) - \varepsilon_2^2\sin(\theta_{12}+\psi)] \tag{38}$$

In the absence of coupling ($r = 0$), the carrier frequency of the two pulses would differ by $\dot{\psi} = \delta/\tau_{RT}$, a frequency difference that can easily be detected by beating the two output pulse trains of the laser (corresponding to either pulse in the cavity) against each other on a detector.

Distributed Backscattering In presence of a sufficient coupling $r \neq 0$, there is generally a solution $\partial\psi/\partial t$ to Eq. (38), such that the two circulating pulses are identical, only differing by a phase factor. If we take for instance the particular case of $\theta_{12} = \theta_{21} = 0$, the constant phase difference is ψ_0 given by

$$\sin \psi_0 = \frac{2\varepsilon_1 \varepsilon_2}{\varepsilon_1^2 + \varepsilon_2^2} \frac{\delta}{2r} \tag{39}$$

Any backscattering such that

$$r \geq \frac{\delta \varepsilon_1 \varepsilon_2}{\varepsilon_1^2 + \varepsilon_2^2} \tag{40}$$

will lock the carrier frequency of the two waves to each other. This implies that the mode frequencies, the repetition rates, and the CEO of the two pulse trains are identical.

Interface Coupling A reciprocal backscattering, where $\theta_{12} = \theta_{21}$ is the norm when dealing with distributed scattering of a solid, liquid, or gaseous medium.[12,13] The situation is different however in a short pulse laser, where the meeting points of the two pulses are localized rather than being distributed over the whole length of the laser resonator. In the case of the mode-locked laser, the backscattering can be due to an interface, in which case $\tilde{r}_{21} = -\tilde{r}_{12}^* = -\tilde{r}^*$; and $\theta_{21} = \theta_{12} + \pi = \theta + \pi$. This type of coupling does not prevent lock-in, since Eq. (38) becomes

$$\frac{\partial \psi}{\partial t} = \frac{\delta}{\tau_{RT}} - \frac{r}{\varepsilon_1 \varepsilon_2 \tau_{RT}} [\varepsilon_1^2 + \varepsilon_2^2] \sin(\theta + \psi) \tag{41}$$

which, for sufficient large r, still has a lock-in solution ψ_0 for which $\partial\psi/\partial t = 0$.

Phase Conjugated Coupling Not all couplings lead to identical mode frequencies of the two output pulse trains of the laser. In a phase conjugated coupling, a fraction r_c of the complex conjugate of one field is coupled into the other field. Such a phase conjugated coupling[14] does preserve the phase identity of each intracavity pulse. The coupled equations for the two pulses are then

$$\begin{aligned} \frac{\partial \tilde{\varepsilon}_1}{\partial t} &= i \frac{\delta}{2\tau_{RT}} \tilde{\varepsilon}_1 + \frac{r_c}{\tau_{RT}} \tilde{\varepsilon}_2^* \\ \frac{\partial \tilde{\varepsilon}_2}{\partial t} &= \frac{r_c}{\tau_{RT}} \tilde{\varepsilon}_1^* - i \frac{\delta}{2\tau_{RT}} \tilde{\varepsilon}_2 \end{aligned} \tag{42}$$

Subtracting the imaginary parts of this equation:

$$\frac{\partial \psi}{\partial t} = \frac{\delta}{\tau_{RT}} \tag{43}$$

and there is no "lock-in" possible with this type of coupling.

Repetition Rate Coupling It has been observed that the repetition rate in both directions can be locked by a saturable absorber. The mechanism by which the average group velocity of the two pulses are locked to each other is described below. This mechanism leaves the carrier frequencies of the two pulses uncoupled.

ULTRASHORT OPTICAL SOURCES AND APPLICATIONS

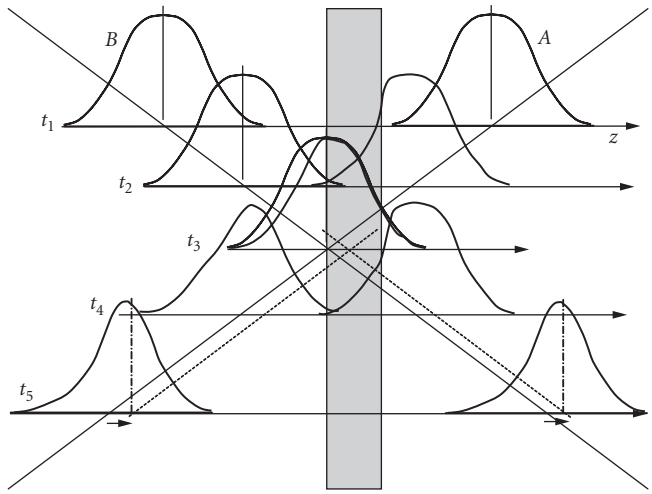

FIGURE 6 Representation of the intracavity pulses entering a saturable absorber. The pulses are plotted as a function of space (z) at successive times. The saturable absorber is initially at the left of the pulse crossing point. Because of mutual saturation, there is only significant absorption when only one of the pulses is present in the absorber. Therefore, the leading edge of pulse A is attenuated more, resulting in an apparent slowing down of the pulse. Similarly, the trailing edge of pulse B is absorbed more, resulting in an apparent acceleration of that pulse. The effect of the absorption combined with mutual saturation is to "pull" the pulse crossing point toward the center of the absorber.

To appreciate this envelope coupling, let us consider a saturable absorber of smaller longitudinal dimensions than the optical pulse, as sketched in Fig. 6. In the figure, the meeting point of the two pulses is on the left of the saturable absorber. Therefore, the pulse A entering from the left enters first the absorber, and its leading edge is attenuated. The absorption is saturated when the two pulses meet in the absorber. The pulse B coming from the left is still partly in the absorber when pulse A has left the absorber. Therefore, its tail will be more absorbed. The net effect is a shift of the center of gravity of both pulses, such that at the next round-trip they will meet closer to the middle of the absorber.

20.5 DESIGNS OF CAVITIES WITH TWO CIRCULATING PULSES

The properties of interwoven intracavity pulses have been discussed in the preceding sections. A few examples of laser cavity designs where two pulses are circulating independently are presented next.

Ring Dye Laser

In a bidirectional ring laser, two pulses circulate in opposite direction. The first realization was a dye laser,[15,16] in which the gain is provided by a jet of Rhodamine 6G in ethylene glycol (pumped by an argon ion laser). A saturable absorber jet of DODCI* has three functions: (i) to mode-lock the laser,

*Di-oxa-di-carbo-cyanide-iodide.

(ii) to ensure bidirectional operation of the laser, and (iii) to define and maintain the pulse crossing point of the envelopes. Bidirectional operation is favored over unidirectional operation because, for the same pulse energy and duration, a single pulse will suffer more intracavity losses than two pulses creating a standing wave by crossing in the absorber.[3] The pulse crossing point is set and maintained by the mechanism just described in Section "Locking Two Pulse Trains by Backscattering". The saturable absorber has to be located approximately 1/4 cavity perimeter ($P/4$) away from the gain jet, in order for each counter-circulating pulse to enter the gain medium at equal time interval ($P/2c$). The phase difference per round-trip between the clockwise (CW) and counter-clockwise (CCW) pulses is measured by combining the CW and CCW pulses on a detector.

Ti:Sapphire Ring Laser with Saturable Absorber

A similar cavity configuration has been used with a Ti:sapphire laser as a gain medium, and a saturable absorber jet of HITCI* for repetition rate synchronization between the two counter-circulating pulses. A sketch of such a cavity is shown in Fig. 7.

The nonlinear index of the gain medium results in a lensing effect, which can be approximated by a positive lens colocated with the gain medium. In mode-locked operation, Kerr lensing induces a positive lens at the location of the gain medium, which modifies the beam size distribution. For the empty cavity, the beam size versus position is represented by the solid line in the graph of Fig. 8. The beams size distribution modified by the self-lensing in the gain rod is indicated by the dotted line in the figure. An aperture located at the position A_1 will favor mode-locked operation, since the losses will decrease with intensity. An aperture located at A_2 will create increasing losses with intensity. This negative feedback stabilizes the mode-locked laser operation. Kerr lensing, which could be considered as an instantaneous saturable absorption,[3] is the technique commonly used to generate the shortest pulses with Ti:sapphire lasers. It is however not a preferred technique for achieving stable bidirectional operation, when, as is typically the case, the active element for Kerr lensing is the gain medium. There is a competition in the gain medium between mutual Kerr lensing, favoring bidirectional operation (with the pulses crossing in the gain medium) and mutual gain saturation favoring unidirectional operation, with the latter generally dominating. An experimental study of a Kerr-lens mode-locked Ti:sapphire laser[18] showed unidirectional operation, switching direction periodically (approximately every 0.1 second). The operation became bidirectional after insertion of a dilute saturable absorber jet inside the cavity.[18]

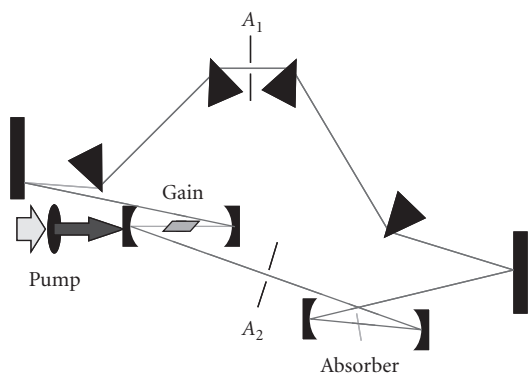

FIGURE 7 Ti:sapphire mode-locked ring laser mode-locked with a saturable absorber jet. Four prisms are used for the control of cavity dispersion.[17]

*Hexa-methyl-indo-carbo-cyanide-iodide.

ULTRASHORT OPTICAL SOURCES AND APPLICATIONS

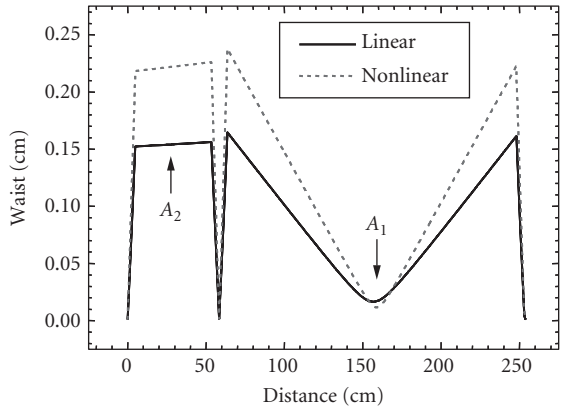

FIGURE 8 Calculation of the cavity mode as a function of position along the cavity, for the empty cavity (solid line) and the cavity modified by nonlinear lensing at the position of the gain medium (dotted line).

The use of a liquid saturable absorber flowing at high velocity (several meters per second) through a narrow nozzle (typically 100 μm thick and 5 mm wide) is essential to ensure the absence of phase coupling between the two pulses. If the saturable absorber were a nonmoving solid, the coupling by scattering would result in a mutual locking of the carrier frequency of the two pulses, as discussed in section "Locking Two Pulse Trains by Backscattering." In the case of the moving fluid of the absorbing dye jet, θ_{12} and θ_{21} are both random functions of time, varying much faster than ψ. Over the time scale that the variation of ψ is negligible, the last terms of Eq. (38) average to zero. Therefore, the dead band has been eliminated, as has been verified experimentally.[19]

Ring Laser with Additional Kerr Crystal

Another technique to achieve bidirectional operation for a Kerr-lens mode-locked laser[20,21] is to insert a nonlinear crystal (for which the nonlinear phase shift is larger than that produced in the gain medium) 1/4 cavity perimeter away from the gain medium. The laser cavity is sketched in Fig. 9.

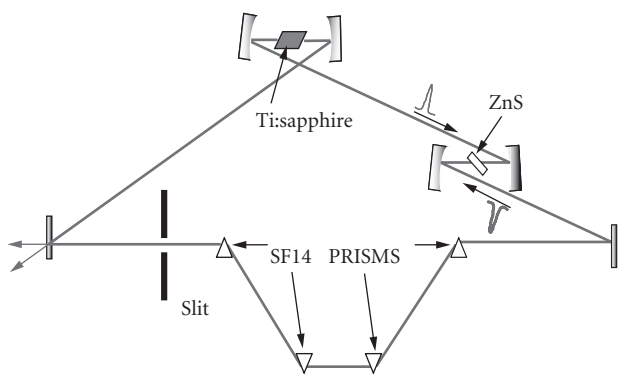

FIGURE 9 Ring laser mode-locked with a nonlinear crystal (ZnS).

The modification to the nonlinear index of refraction due to two counter-propagating fields of direction i and j is

$$n_2^i = n_2(I_i + 2I_j) \tag{44}$$

The factor 2 on the right hand side of Eq. (44) reflects the well-known act that cross-phase modulation is twice as effective as self-phase modulation for the same intensity.[22] Assuming equal intensity in the counter-propagating fields and similar waists for single pulse operation versus bidirectional operation yields the following approximate relationship for the nonlinear index of refraction in the ZnS crystal for single pulse (unidirectional) versus double pulse (bidirectional) operation:

$$\Delta n_{\text{bidirectional}} \sim \frac{3}{2}\Delta n_{\text{single}}\left[\frac{\text{interaction length}}{\text{crystal length}}\right] \tag{45}$$

Because the overlap region of the pulse envelopes is approximately the pulsewidth/c, the mutual Kerr-lens will dominate only if the length of the Kerr medium is not much longer than the pulsewidth. Depending on the pulsewidth and crystal thickness, there may be enough nonlinearity to distinguish between single-pulse operation and bidirectional operation. To enhance the mutual Kerr effect, a crystal of ZnS was chosen, because its nonlinear index is 50 times larger than that of Ti:sapphire.[21] Pulses as short as 60 fs were generated, meeting in the ZnS crystal used as a nonlinear element. Because the two countercirculating pulses have different intensities, a differential phase shift between the two directions results in a difference of cavity modes of 60 kHz. In addition to the relative shift of the modes, this laser system has the additional complexity that the center of spectral envelope of either countercirculating pulse is shifted by 2 nm.

Imperfection in the ZnS crystal used as nonlinear element resulted in coupling of the beams by scattering. The amount of coupling can be measured through the spectrum of the beat note of the two pulse trains. Such a spectrum shows for instance a fundamental at 60 kHz and harmonics at 120 kHz and 180 kHz. Such a spectrum can lead to the lock-in frequency between the two beams,[23] which in the case of the experiment cited is 1.8 kHz.[21]

Linear Lasers

Considering the ring laser sketched on the top of Fig. 7, it is possible to visualize stretching the cavity by the two mirrors at the extreme left and right, while keeping the perimeter constant. The limit of the stretched out ring is a linear cavity in which two pulses circulate.

As an example, let us consider a linear cavity used to measure with high accuracy the electro-optic coefficient.[24] The laser cavity is similar to the typical linear cavity mode-locked Ti:sapphire laser, but with a saturable absorber (a jet of HITCI dye dissolved in ethylene gylcol) placed in the center of the cavity, as sketched in Fig. 10. As in the case of the ring laser discussed above, Kerr-lens mode-locking does not appear to be possible with double pulse operation. Instead, a saturable absorber is positioned in the middle of the cavity by translating one of the end mirrors. The distance that the end mirror can be translated while maintaining double pulses is about 2 cm, in excess of the pulse length of approximately 0.6 mm (2-ps pulses). The 2-cm distance is a 120-ps delay and corresponds to the lifetime of the dye. The dye concentration is not a critical parameter and can be varied over a broad range without affecting the performance of the laser. The 140-MHz output from one end of the laser, detected on a fast photodiode, is filtered, its frequency divided by 2 in an ECL logic. The resulting 70-MHz signal is which yielded a 70-MHz sinusoidal signal. Finally the signal is amplified again and applied to synchronize the measurement to be performed. In the case of measurement of an electro-optic coefficient, the 70-MHz signal is applied directly to electrode on the crystal to be measured, in parallel with a 50-ohm terminator.[24]

Whether to use a ring or linear cavity depends on the quantity to be measured. The ring laser is sensitive to rotation, and to fresnel drag in one of its arms.[25] Without any rotation or modulation a

ULTRASHORT OPTICAL SOURCES AND APPLICATIONS

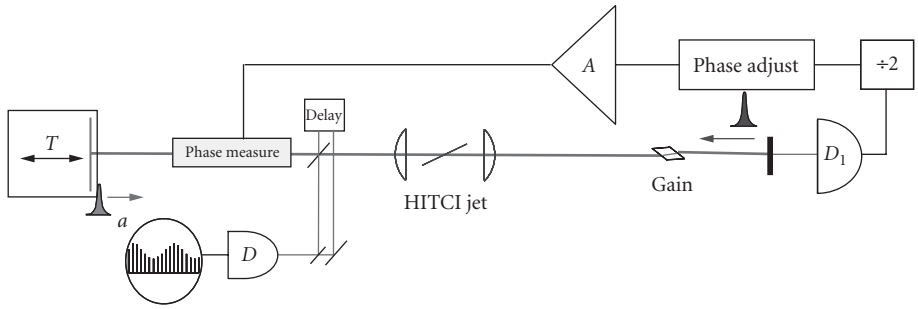

FIGURE 10 Linear laser mode-locked with a saturable absorber to produce two pulses/cavity round-trip. The end mirror on the left is on a translation stage *T*, in order to set the position of the saturable absorber in the middle of the cavity. The saturable absorber is a jet of HITCI dissolved in ethylene glycol, between two focusing elements. The output pulse train, recorded on a photodiode, reduced to half frequency, is used to synchronize a phase measurement. Each of the two intracavity pulses experience a different phase shift per round-trip, hence a different carrier frequency. The two intracavity pulses are extracted from the cavity with a beam splitter, and recombined after an appropriate optical delay. The two interfering pulse trains show a beat signal on the detector *D*.

mode-locked ring laser normally has a beat frequency offset of at least 100 Hz and often as high as 100 kHz.[26] This is a result of the asymmetry in the CW and CCW pulse. Because of the nonlinear intracavity elements, the order in which the pulse encounters the optical elements will affect the pulsewidth and pulse amplitude.[3,27,28] Any variation in pulse amplitude or pulsewidth will be seen as a beat signal. Since the pulses in a linear cavity travel through the same optical elements in the same order, there is no asymmetry. Therefore, one advantage of a linear cavity versus a ring geometry is the improvement in the frequency offset.

As the electronic delay of the signal applied to the sample is varied, the beat note shows a sinusoidal dependence, as shown in Fig. 11, which is a plot of the beat frequency versus the delay. The optimum timing occurs when one pulse sees a voltage on the sample of $+V_0$ and the second pulse sees a voltage of $-V_0$ at the sample. The line plotted in Fig. 11 is not a fit, but a plot of $V_0\left|\sin\left(\frac{2\pi c}{2L}\tau-\phi_0\right)\right|$, where the fixed phase ϕ_0 was the only free parameter.

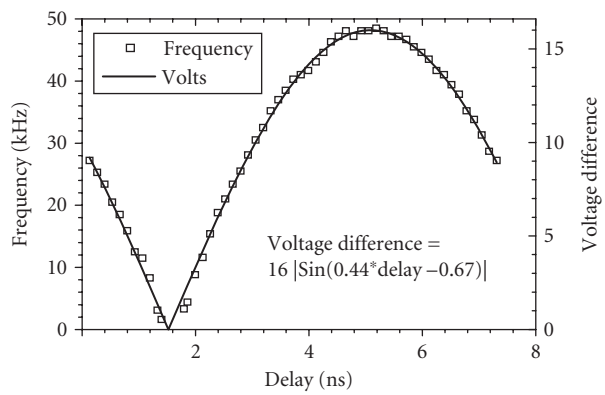

FIGURE 11 Delay dependence of the beat note frequency.

Optical Parametric Oscillators

The coupling between oppositely circulating beams in a ring laser is eliminated if a laser operates with ultrashort pulses* circulating in opposite direction and crossing in a nonscattering medium such as vacuum or air. It is however quite a challenge to find means to couple the pulse envelopes, without introducing any phase coupling. One solution described in the previous sections is to couple the pulses in amplitude in a medium that moves transversally to the beam, such as a jet of liquid saturable absorber. Another solution is the synchronously pumped optical parametric oscillator (OPO), which offers the possibility to decouple relative phase and repetition rates of the oscillating signals, without the need for any moving element.

A simple configuration is that of an OPO-pumped extracavity by a Ti:sapphire mode-locked laser, as sketched in Fig. 12. The position of the crossing point of the two circulating pulses in the OPO is simply determined by the timing of the pump pulses, rather than by a saturable absorber[19] or a nonlinear crystal.[21] The mode frequencies are still set by the cavity. Another advantage over other systems is the tunability, which is important for applications such as detecting ultra low magnetic fields, where the laser radiation has to be tuned to a narrow atomic transition.

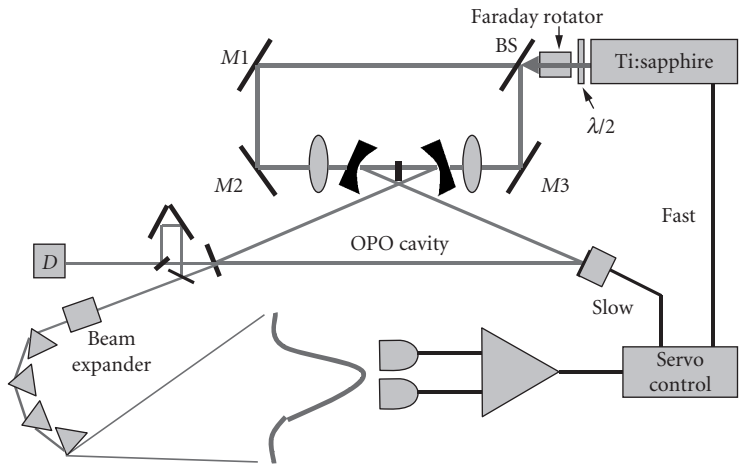

FIGURE 12 Illustration of the OPO cavity pumped by the Ti:sapphire laser. The reflected and transmitted parts of the beam splitter BS are focused into the periodically poled lithium niobate crystal via the two branches of an antiresonant ring. The beams should destructively interfere at the antiresonant ring output, which is monitored with a CCD. Since all the radiation is, in exact alignment, reflected back into the laser, a two-stage optical isolator is required to prevent disruption of the mode-locked operation. The nonlinear crystal is a 0.8-mm-long periodically poled lithium niobate (PPLN) crystal with a period of 19.75 μm, temperature stabilized at 353 K to prevent photorefractive damage and achieve quasi-phase-matching condition for generation of a signal of 1.35 μm with an average power of 30 mW per direction. The difference between the two optical paths from the beam splitter to the crystal determines the crossing point of the signal pulses in the OPO cavity. The two output pulses are made to interfere on a detector D after an optical delay line brings them in coincidence. A four-prism sequence sends the pulse spectrum onto a pair of detectors. The difference between the two detected signals is amplified and applied to a piezo to stabilize the cavity length.

*Pulse duration τ in the range from femtoseconds to a few picoseconds, pulse length $C\tau$ much shorter than any linear dimension in the cavity.

ULTRASHORT OPTICAL SOURCES AND APPLICATIONS

A periodically poled $LiNbO_3$ crystal (PPLN) is excited by a "pump pulse" at an optical frequency ω_p to provide gain at a "signal" frequency ω_s through the process $\omega_p = \omega_s + \omega_i$ where ω_i is the "idler." The OPO is an oscillator which uses the gated gain at ω_s. Therefore, as opposed to a conventional gain medium, in an OPO, the timing, direction, and position of the gain are determined by the time of arrival, k vector and focal spot location of the pump pulse in the parametric crystal. A Ti: sapphire laser provides a train of gating pump pulses of 200-fs duration at 789 nm, 143-MHz repetition rate, and 400-mW average power. The cavity of the pump laser is in a ring configuration, and operates unidirectionally. Such a configuration is less sensitive to feedback than a linear cavity. A double stage Faraday isolator (providing −60-db isolation) is still required to prevent the feedback from the OPO antiresonant ring pumping arrangement (Fig. 12)[29,30] from destroying the mode-locked operation. The sensitivity of the OPO wavelength to cavity mismatch can be exploited to stabilize the synchronously pumped OPO. Indeed, since the repetition rate of the OPO is fixed by the pump laser, the signal wavelength will adjust to a value for which the round-trip rate matches the pump rate.[31,32] As a result, any fluctuation of OPO cavity length relative to that of the pump cavity will be translated into a change in wavelength of the OPO laser. In the arrangement skeched in Fig. 12, motions of the spectrum are detected by spectrally dispersing (with 4 prisms) an expanded output from the counter-clockwise OPO beam. The signal spectrum, centered at 1.35 μm, is split into two parts and collected by a pair of lenses into two infrared photodiodes (Fig. 12). The difference signal of the two detectors monitoring two spectral components on either side of the pulse spectrum is sent through a high-gain amplifier ($\omega_{3db} = 1$ kHz) to drive piezoelectric transducers (PZT) translating an OPO (slow servo loop) and a Ti:sapphire mirror (fast servo loop).

The beat note observed with the configuration of Fig. 12 has a bandwidth of tens of kilohertz,[33] because of the extreme (nanometer) sensitivity of the OPO to the pump spot position, as demonstrated experimentally in reference.[34] The beat note bandwidth is thus fundamentally due to fluctuations in the gain spot position for either circulating pulse, due to the beam pointing instability of the pump laser. The basic remedy is to make the two pump spots part of the same spatial mode of a cavity. One solution that has been implemented[34] is to insert the OPO crystal inside the cavity of the pump laser. Implementation of an OPO pumped intracavity by a linear Ti:sapphire laser is shown in Fig. 13. Four LaKL21 prisms are incorporated in the pump cavity to compensate the group velocity dispersion (GVD) from the Ti:sapphire crystal, the PPLN crystal, and other intracavity elements such as lenses and mirrors. This four-prisms configuration was necessitated by the desire to have large GVD compensation (needed because of the large positive GVD of $LiNbO_3$) and a reasonably short cavity length (1/2 of the perimeter of the OPO cavity). Two quantum wells (MQW) of AlGaAs on top of a mirror structure are used in the cavity as a saturable absorber to mode-lock the laser. The

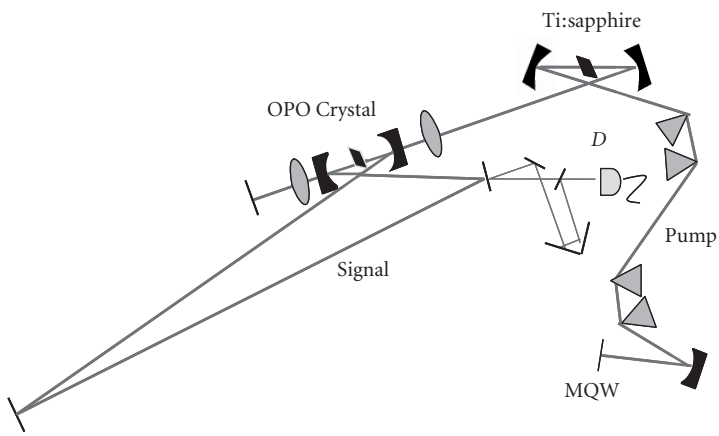

FIGURE 13 Illustration of the intracavity OPO pumped by the Ti:sapphire laser. The main control of the GVD compensation is the prism spacing L_2.

Ti:sapphire laser radiation consists of 200-fs pulses centered at 785 nm, repetition rate of 95 MHz. The OPO crystal is a 3-mm-long Brewster cut PPLN crystal (HC Photonics, Taiwan) with a period of 19.4 μm (quasi-phase matching for signal near 1.36 μm), which is temperature stabilized at 408 K to prevent photorefractive damage. Attempts to use OPO crystals cut near normal incidence and antireflection coated failed, because the Ti:sapphire mode-locked operation was prevented by the smallest feedback from the antireflection coating. This feedback problem was completely eliminated through the use of a Brewster angle cut, but at the price of a considerably more difficult alignment procedure. Because of the Brewster angle cut of $LiNbO_3$, the idler, the pump radiation and its second harmonic all exited the crystal at a different angle, and could not be used for alignment of the OPO cavity (the OPO cavity mirrors were reflecting at the signal wavelength of 1.4 μm and at the second harmonic of the pump).

20.6 ANALOGY OF A TWO-LEVEL SYSTEM

In the previous section, some methods for mode-locking a laser with two intracavity pulses were described. Inside the cavity, these two pulses can couple to each other in diverse ways which were analyzed in Sec. 20.4. The purpose of circulating two pulses in a laser cavity is that intracavity perturbations created by the quantity to be measured will alter the carrier frequency of a pulse, a shift in frequency that can easily be detected by interfering the output pulse trains. The laser itself is used as an interferometer, with the remarkable properties that the phase shift occurring in the cavity is transformed in a frequency shift. There are numerous factors influencing the accuracy as well as the sensitivity of a measurement performed intracavity. A better understanding of the two pulse per cavity laser can be reached by noting the complete analogy with a quantum mechanical two-level system. In the quantum mechanical situation an atomic or molecular system can be in one or two quantum states $|k\rangle$, with $k = 1$ and 2, of energy $\pm\omega_0/2$. Each of these states correspond to pulse $|2\rangle$ and pulse $|2\rangle$ in the laser cavity. For instance, in a ring laser, one of the states would correspond to a counterclockwise circulating pulse, the other to the clockwise circulating pulse. The interaction of a two-level system with a near resonant field is the most thoroughly studied problem in atomic and molecular physics. Techniques developed to achieve sublinewidth resolution in atomic physics may be transposed to the laser situation, and, thanks to the analogy, lead to methods to enhance the resolution of intracavity laser sensors.

Review of Coherent Interaction of Two-Level Systems

Considering the case of two level with a dipole allowed transition, in presence of a near resonant electromagnetic field $E = 1/2\tilde{\varepsilon}(t)\exp(i\omega t) + \text{c.c.}$ In presence of this electric field, the state of the atomic/molecular system is described by the wavefunction ψ, a solution of the time-dependent Schrödinger equation:

$$H\psi = i\hbar\frac{\partial\psi}{\partial t} \tag{46}$$

with the total Hamiltonian given by

$$H = H_0 + H' = H_0 - p\cdot E(t) \tag{47}$$

where p is the dipole moment. In the standard technique for solving time dependent problems, the wave function ψ is written as a linear combination of the basis functions $|k\rangle$:

$$\psi(t) = \sum_k a_k(t)|k\rangle \tag{48}$$

This expression for ψ is inserted in the time dependent Schrödinger Eq. (46). Taking into account the normalization conditions for the basis functions ψ_k, one finds the coefficients a_k have to satisfy the following set of differential equations:

$$\frac{da_k}{dt} = -i\omega_k a_k + \sum_j \frac{i}{2\hbar} p_{k,j} [\tilde{\varepsilon} e^{i\omega_\ell t} + \tilde{\varepsilon}^* e^{-i\omega_\ell t}] a_j \tag{49}$$

where $p_{k,j}$ are the components of the dipole coupling matrix for the transition $k \to j$, and a_k are the amplitudes of the eigenstates. Phase and amplitude relaxation have been neglected so far and will be introduced later. It should be noted that Eq. (49) is of a quite general nature, is ideally suited to numerical integration, and is not limited to two level systems. Similarly, the laser analogy can be extended to lasers with more than two intracavity pulses. We will consider here only two levels, with a very small detuning $\Delta\omega = \omega_0 - \omega \ll \omega_0$:

$$\Delta\omega = \omega_0 - \omega \tag{50}$$

Consistent with the approximation of small detuning, we replace the set of coefficients a_k, which have temporal variations at optical frequencies, by the "slowly varying" set of coefficients c_k, using the transformation:

$$a_k = e^{-ik\omega_\ell t} c_k \tag{51}$$

Inserting in the pair of Eqs. (49), leads to the pair of differential equations for the two coefficients c_k:

$$\frac{d}{dt}\begin{pmatrix} c_1 \\ c_2 \end{pmatrix} = \begin{pmatrix} i\frac{\Delta\omega}{2} & i\frac{1}{2}\frac{p}{\hbar}\tilde{\varepsilon} \\ -i\frac{1}{2}\frac{p}{\hbar}\tilde{\varepsilon}^* & -i\frac{\Delta\omega}{2} \end{pmatrix}\begin{pmatrix} c_1 \\ c_2 \end{pmatrix} \tag{52}$$

where $\kappa|\tilde{\varepsilon}| = (p/\hbar)|\tilde{\varepsilon}|$ (p being the dipole moment of the single photon transition) is the Rabi frequency.

The Laser as a Two-Level System

The two-level system considered above is isolated, hence the total population is conserved. The analogue of the electromagnetic field coupling states $|1\rangle$ and $|2\rangle$ is a conservative intracavity coupling $\tilde{r}_{12} = -\tilde{r}_{21}^*$. Such a type of coupling can only be considered in the case of mode-locked lasers, where the localization of the radiation in the cavity enables one to select a truly conservative coupling. The coupling, localized at the crossing point of the two circulating pulses, can be produced by the backscattering at a dielectric interface† between two media a and b, for which $\tilde{r}_{ab} = \tilde{r}$ and $\tilde{r}_{ba} = -\tilde{r}^*$. It can easily be verified that the total intensity change introduced by this coupling is zero, as expected for a conservative coupling. In fact, the phase relation between the two reflections at either sides of the interface is a consequence of energy conservation.

In the analogy of the laser, the coefficients $c_i(t)$ correspond to the complex field amplitudes $\tilde{\varepsilon}_i$ (the tilde indicating a complex quantity) of each pulse circulating in the ring cavity (round-trip

†In the case of a linear laser with two pulses/round-trip, the conservative coupling is only possible when there are two crossing points in the cavity, and that the interface is located at one of the crossing points.

time τ_{RT}). The state of the system is also defined by $\psi(t)=\tilde{\varepsilon}_1(t)|1\rangle+\tilde{\varepsilon}_2(t)|2\rangle$. The evolution equation of these fields are

$$\frac{d}{dt}\begin{pmatrix}\tilde{\varepsilon}_1\\ \tilde{\varepsilon}_2\end{pmatrix}=\frac{1}{\tau_{RT}}\begin{pmatrix}\tilde{r}_{11} & \tilde{r}_{12}\\ \tilde{r}_{21} & \tilde{r}_{22}\end{pmatrix}\begin{pmatrix}\tilde{\varepsilon}_1\\ \tilde{\varepsilon}_2\end{pmatrix}=\frac{1}{\tau_{RT}}||R||\cdot||E|| \tag{53}$$

In order to have an equivalence between Eqs. (52) and (53), the matrix $||R||$ should be *Anti-Hermitian*, which, in addition to the condition $\tilde{r}_{21}=-\tilde{r}_{12}^*$, imposes and that $\tilde{r}_{kk}$ be purely imaginary. It can also easily be verified that this is the only form of interaction matrix for which energy is conserved $d/dt\left(|\tilde{\varepsilon}_1|^2+|\tilde{\varepsilon}_2|^2\right)=0$. The real parts of the diagonal elements of the matrix $||R||$ represent gain and loss in the cavity. In steady state, the gain and loss are in equilibrium, and the real parts of $\tilde{r}_{kk}$ are zero. A gain (or absorber) with a recovery (relaxation) time longer than $\tau_{RT}/2$ will cause transients in population. The laser equivalent to the detuning $\Delta\omega$ is a differential phase shift for the pulses $|1\rangle$ and $|2\rangle$ in the cavity. Such a differential phase shift is introduced either by rotation in a ring laser,[15,16] or with an electro-optic modulator in a linear laser.[24] In the latter case, the electro-optic phase modulator imposes an opposite phase shift ($\Delta\phi/2$ and $-\Delta\phi/2$) for either pulse, thereby modifying the resonance of the cavity for the pulse $\tilde{\varepsilon}_1$ by $\Delta\omega/2=\Delta\phi/(2\tau_{RT})$, and for pulse $\tilde{\varepsilon}_2$ by $-\Delta\omega/2=-\Delta\phi/(2\tau_{RT})$. These detuning terms contribute to the diagonal terms of the matrix $||R||$: $\tilde{r}_{11}=-\tilde{r}_{22}=i\Delta\phi/2$.

The analogy between the laser and a two-level system applies also to the set of density matrix equations. These can be obtained by rewriting Eq. (53) in terms of the intensities in either sense of rotation $\rho_{22}=\tilde{\varepsilon}_2\tilde{\varepsilon}_2^*$ and $\rho_{11}=\tilde{\varepsilon}_1\tilde{\varepsilon}_1^*$, and the quantities $\rho_{12}=\tilde{\varepsilon}_1\tilde{\varepsilon}_2^*$ and $\rho_{21}=\tilde{\varepsilon}_2\tilde{\varepsilon}_1^*$:

$$\frac{d(\rho_{22}-\rho_{11})}{dt/\tau_{RT}}=-4\mathrm{Re}(\tilde{r}_{12}\rho_{21})-\frac{(\rho_{22}-\rho_{11})}{T_1} \tag{54}$$

$$\frac{d\rho_{21}}{dt/\tau_{RT}}=-i\Delta\omega\tau_{RT}\rho_{21}+\tilde{r}_{12}^*(\rho_{22}-\rho_{11})-\frac{\rho_{21}}{T_2} \tag{55}$$

where, as in the case of the two-level system interacting with a near resonant field, phenomenological relaxation times T_1 and T_2 have been introduced. One recognizes here Bloch's equation for a two-level system driven off-resonance by a step function Rabi frequency of amplitude $\tilde{r}/\tau_{RT}$.[35] The difference in intensities $(\rho_{22}-\rho_{11})$ is the direct analogue of the population difference between the two levels. The off-diagonal matrix element ρ_{21} is the interference signal obtained by beating the two outputs of the laser on a detector. As in the case of the two-level system, one can introduce phenomenological relaxation times T_1 for the energy relaxation (diagonal matrix element) and T_2 for the coherence relaxation (off-diagonal matrix elements). As for the quantum mechanical two-level system, $1/T_2$ is the homogeneous component of the linewidth of the beat note between the two pulse trains. There is also an "inhomogeneous" component to that linewidth, which has as physical origin the mechanical vibration of the laser components, causing random fluctuations of the beat note. Because of mechanical vibrations, each pulse sees random differences in the cavity length caused by mirror motion over a time of $\tau_{RT}/2$).

Table 1 summarizes the main points of the analogy between a laser with two pulses/cavity and the coherent interaction of a two-level system with a near resonant electromagnetic field.

Experimental Demonstration of the Analogy

The most typical manifestation of a two-level system interacting with a step function electromagnetic pulse is Rabi cycling, which is a periodic transfer of population from one state to the other. To observe such a periodic transfer, the system should be in one of the two states at $t=0$. One method to prepare the ring laser with one state (direction) dominating, is to feedback one direction into the other outside of the cavity (Fig. 14). The output pulse from one direction is extracted, and fed back (<1 percent) with a mirror, after appropriate optical delay, into the opposite direction. By using a fast switch (turn-off time of less than the cavity round-trip time of 10 ns) at the Pockel's cell, the coupling can be turned off, to let the counter-circulating fields evolve in the cavity.

TABLE 1 Summary of the Analogy between a Two-Level System and the Laser with Two Circulating Intracavity Pulses

	Two-Level System	Laser
Basic states	$\|k\rangle; k=1,2$	$\|k\rangle k=1,2$
corresponding to	energy level $\pm\frac{\omega_0}{2}$	Intracavity pulses 1, 2 selected by geometry
Coupling through	Near-resonant E-field at ω	Backscattering at interface
Detuning	$\Delta\omega=\omega_0-\omega$	$\Delta\omega=\Delta\phi\,\tau_{RT}$
Slowly varying	$\Delta\omega<<\omega$	$\Delta\omega<<1/\tau_{RT}$
Wave function	$\psi(t)=a_1(t)\|1\rangle+a_2(t)\|2\rangle$	$\psi(t)=\varepsilon_1(t)\|1\rangle+\varepsilon_2(t)\|2\rangle$
Density matrix	$\rho_{kk}-a_k a_k^*$ Populations	$\rho_{kk}=\tilde{\varepsilon}_k\varepsilon_k^*$ (Intensities)
elements	$\rho_{kk}=-a_i a_j^*$	$\rho_{ij}=\tilde{\varepsilon}_i\varepsilon_i^*$ (beat signal)

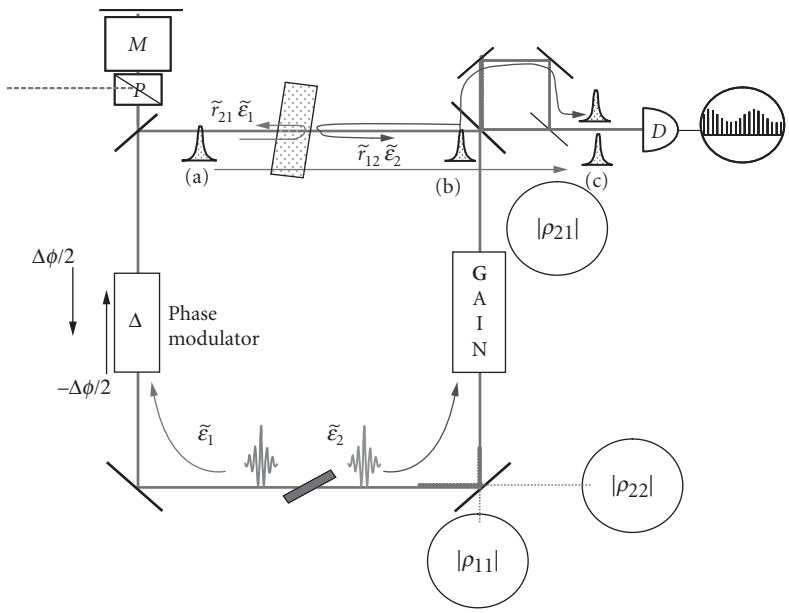

FIGURE 14 Sketch of the ring laser used to demonstrate the analogy with a two-level system. In the bidirectional mode-locked ring laser two circulating pulses meet in a saturable absorber jet. Three successive positions: (a), (b), and (c) of the two pulses are shown. An interface, positioned at or near the opposite crossing point of the two pulses, controls the amplitude of the coupling parameter $\tilde{r}_{ij}$. The circulating intensities in the laser, measured for each direction by quadratic detectors, are the diagonal elements (populations) of the density matrix of the equivalent two-level system. The absence of phase modulation corresponds to the two levels being on resonance, driven at the Rabi frequency $(p/\bar{h})\varepsilon$ by a resonant field (the Rabi frequency $(p/\bar{h})\varepsilon=\kappa\varepsilon$ corresponds to the frequency r_{12}/τ_{RT} in the ring laser analogy). The backscattering at the interface provides thus coherent coupling (Rabi cycling) between the two states, while other noncoherent decays tend to equalize the population in the two directions, and washes out the phase information. The detuning $\Delta\omega$ corresponds to the phase difference per round–trip $\Delta\phi/\tau_{RT}$, imposed by an electro-optic phase modulator driven exactly at the cavity round-trip time. A beat-note detector measuring the interference between the two fields, records the off-diagonal matrix element. A combination of a Pockel's cell M and polarizer P controls a feedback of the clockwise pulse into the counterclockwise one.

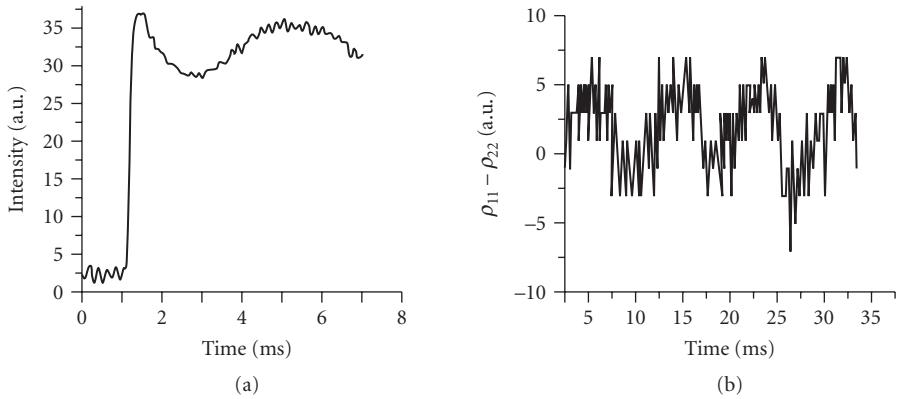

FIGURE 15 The evolution of the intensities are shown after switching the Pockels' cell. (*a*) The counterclockwise direction is shown—the intensity at clockwise direction is 180° out of phase with this graph, with population dropping from the maximum initial value. The fast initial transient reflects the gain and cavity dynamics associated with the sudden change in cavity loss at the switching time. Thereafter, a slow oscillation due to population transfer or Rabi oscillation between two directions is observed. (*b*) Population difference showing the Rabi cycling.

Rabi Cycling on Resonance In the measurements that follow, the system is "at resonance"; (i.e., $\Delta\omega = 0$). An example of "Rabi cycling" is shown in Fig. 15. The counterclockwise intensity (ρ_{22}) is plotted as a function of time [(Fig. 15*a*)]. The clockwise intensity ρ_{11} (not shown) is complementary. The system is prepared so that the ρ_{11} is initially populated ($\rho_{11} = 0.8, \rho_{22} = 0.2$). As the feedback that creates the initial state is switched off at $t = 1$ ms, there is a fast (approximately 10 μs) transient. This risetime reflects combined dynamics of the gain and cavity, as the laser adapts to the different (now symmetrical) cavity losses. This risetime corresponds roughly to the fluorescence lifetime of the upper state of Ti:sapphire. The "Rabi cycling" of the "population difference" $\rho_{22} - \rho_{11}$ is plotted in Fig. 15*b*. One can also record the beat note frequency (off-diagonal element $|\rho_{12}|$) as sketched in Fig. 14. As can easily be seen from the Bloch vector model of Feynman et al.,[35] the oscillation of the diagonal elements and the off-diagonal elements are 90° out of phase. This property can indeed be seen in Fig. 16*a*. The Rabi frequency $|\tilde{r}|/\tau_{RT}$ can be varied by changing the position of the scattering surface, as shown in Fig. 16*b*. The maximum value measured[36] for this interface corresponds to a

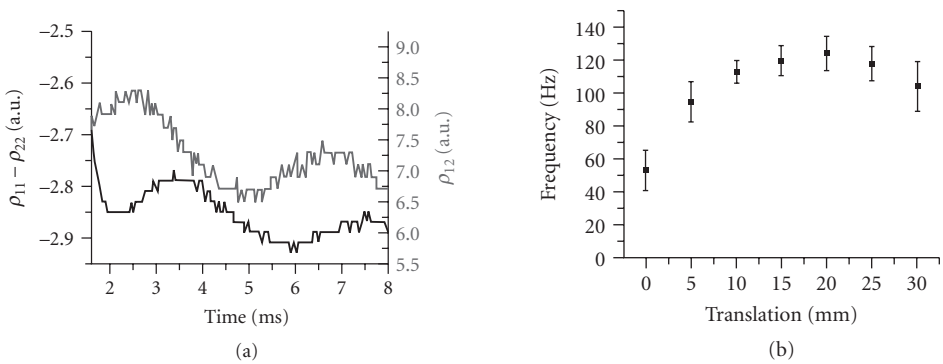

FIGURE 16 (*a*) Comparison of the oscillation of the population difference $\rho_{22} - \rho_{11}$ and the off-diagonal element (beat note) ρ_{12}. (*b*) Rabi frequency as a function of position of the glass at the meeting point of the two directions. Translation of the glass-air interface along the beam results in different values of coupling $\tilde{r}$.

ULTRASHORT OPTICAL SOURCES AND APPLICATIONS

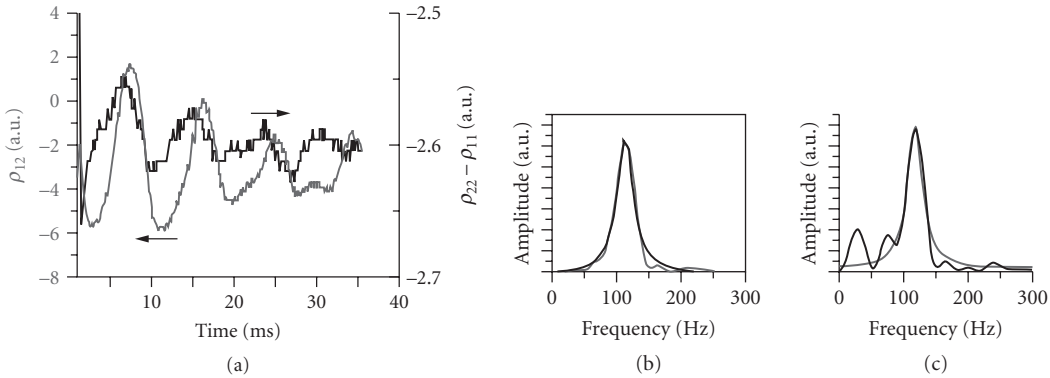

FIGURE 17 (*a*) Measurement of the decay of the Rabi oscillations $\rho_{22} - \rho_{11}$ and ρ_{21}. (*b* and *c*) The Fourier transforms of the relative measurements are shown on the right.

backscattering coefficient of $|\tilde{r}| \approx 1 \cdot 10^{-6}$. Note that the Rabi frequency provides a direct measurement of very minute backscattering coefficients, without the need to trace a complete gyroscopic response as in Refs. 36 and 37.

In the case of a two-level system, the phenomenological "longitudinal" and "transverse" relaxation times have been identified as energy relaxation time (fluorescence decay) and phase relaxation time (due for instance to atomic collisions). Figure 17 shows a measurement of the decay of the Rabi oscillation for the diagonal and off-diagonal elements. The decay is measured by fitting the Fourier transform of the measurement to a Lorentzian, and measuring its FWHM. The values are 27 and 30 Hz. As noted previously, there are at least two origins to the decay of the off-diagonal element: vibration of mirrors, and coupling through absorption (gain). The latter affects equally the diagonal and off-diagonal elements. The former can be seen as a type of "inhomogeneous broadening," since it has its origin in random cavity length fluctuation, expressed as randomness in the value of $\Delta\omega$. The approximately 30-Hz bandwidth of both decays is consistent with 0.3-μm amplitude vibrations at 100 Hz of cavity components, causing differential cavity fluctuations of 0.3 pm/round-trip.

The role of the gain coupling is particularly important in the present Ti:sapphire laser because of the long-gain recovery time. A better candidate for this analogy would be a dye or semiconductor laser for which the gain lifetime is shorter than the cavity round-trip time. An OPO provides an even better situation, since the gain exists only at the time of pumping.

Rabi Cycling Off-Resonance

If the radiation of amplitude ε (Rabi frequency $\kappa\varepsilon$) is off-resonance with a two-level system by an amount $\Delta\omega$, the Rabi frequency becomes $\sqrt{\kappa^2\varepsilon^2 + \Delta\omega^2}$. In the case of the ring laser, we can control the off-resonance amount $\Delta\omega$ with a Pockel's cell (Fig. 14), the initial condition is set favorable to the counter-clockwise direction as shown in Fig. 15*a*. The Rabi cycling is measured indeed to correspond to $\sqrt{|\tilde{r}|^2/\tau^2 + \Delta\omega^2}$. In resonance case $\Delta\omega = 0$), measurement of ρ_{12} leads to $r/\tau_{RT} = 138\,\text{Hz} \pm 15\,\text{Hz}$. With $\Delta\omega$ of $171\,\text{Hz} \pm 12\,\text{Hz}$, the off-resonant measurement is $r/\tau_{RT} = 237\,\text{Hz} \pm 21\,\text{Hz}$, which follows the behavior of an off-resonance two-level system.

Impact of the Analogy

The analogy between two-level and laser systems may be more than just a scientific curiosity. A thorough understanding of two-level systems led to powerful spectroscopic techniques, using sophisticated

pulse sequences. Rather than using optical pulses, sublinewidth molecular spectroscopy has been successfully realized by pulsing the detuning by the Stark shifts.[38–40] In the case of the ring laser, similar pulse sequences can be applied to the detuning. The information sought in spectroscopy is contained in the measurement of $|\rho_{12}|$, as a function of the driving field (measurement of the Rabi frequency $\kappa\varepsilon$ leading to the determination of the dipole moment) or detuning $\Delta\omega$. In the case of the ring laser, the measurement of $|\rho_{12}|$ is linked to the properties of some sample inserted in the cavity.[11] Any resolution enhancing technique that has been devised in spectroscopy, such as the Ramsey fringes,[41, 42] could be transposed to a laser phase sensor with two intracavity pulses.

20.7 CONCLUSION

This chapter started with a mathematical description of short optical pulses and optical pulse train. Basic physics of short pulse generation in a mode-locked laser are discussed. It is shown in particular that the mechanism by which a steady-state pulse is generated inside the laser, is also responsible for creating equally spaced modes in the frequency domain. It is shown that pulse train interferometry combines the properties of temporal and spatial resolution. The laser can be used as a most sensitive interferometer, when the reference and sample pulses are circulating in the same cavity. Measurements of extreme sensitivity can be performed by interfering the two pulse trains emitted by such a laser. The exquisite sensitivity to phase results from the fact that a phase shift is transposed into a frequency shift inside the active cavity. Exploitation of such lasers as sensors requires a thorough understanding of the coupling between the two intracavity pulses. A new modeling of the laser with two intracavity pulses is introduced by making an analogy with a quantum mechanical two-level system. Beyond its physical elegance, this analogy inspires new sensitivity enhancement techniques for the use of the two-pulse per cavity laser sensor.

20.8 REFERENCES

1. Ladan Arissian and Jean-Claude Diels. "Carrier to Envelope and Dispersion Control in a Cavity with Prism Pairs." *Phys. Rev. A* **75:**013814–013824, 2007.
2. F. X. Kärtner, N. Matuschek, T. Schibli, U. Keller, H. A. Haus, C. Heine, R. Morf, V. Scheuer, M. Tilsch, and T. Tschudi. "Design and Fabrication of Double Chirped Mirrors." *Opt. Lett.* **22:**831–833, 1997.
3. J.-C. Diels and Wolfgang Rudolph. *Ultrashort Laser Pulse Phenomena,* 2d ed. Elsevier, Boston, 2006, ISBN 0-12-215492-4.
4. Th. Udem, J. Reichert, R. Holzwarth, and T.W. Hänsch. "Accurate Measurement of Large Optical Frequency Differences with a Mode-Locked Laser." *Opt. Lett.* **24:**881–883, 1999.
5. J.-C. Diels. Femtosecond Dye Lasers. In F. Duarte and L. Hillman, (eds.) *Dye Laser Principles: With Applications,* Academic Press, Boston, 1990. ISBN 0-12-215492-4, chapter 3, pages 41–132.
6. C. M. Depriest, T. Yilmaz, P. J. Delfyett, S. Etemad, A. Braun, and J. H. Abeles. "Ultralow Noise and Supermode Suppression in an Actively Mode-Locked External-Cavity Semiconductor Diode Ring Laser." *Opt. Lett.* **27:**719–721, 2002.
7. B. Resan and P. J. Delfyett. "Dispersion-Managed Breathing-Mode Semiconductor Mode-Locked Ring Laser: Experimental Characterization and Numerical Simulations." *IEEE J. of Quantum Elect.* **40:**214–220, 2004.
8. T. Yilmaz, C. M. Depriest, and P. J. Delfyett. "Complete Noise Characterisation of External Cavity Semiconductor Laser Hybridly Modelocked at 10 ghz." *Elect. Lett.* **22:**1338–1339, 2003.
9. T. Yilmaz, C. M. Depriest, A. Braun, and J. H. Abelesand P. J. Delfyett. "Residual Phase Moise and Longitudinal Mode Linewidth Measurements of Hybridly Modelocked External Linear Cavity Semiconductor Laser." *Opt. Lett.* **27:**872–874, 2002.
10. T. Yilmaz, C. M. Depriest, A. Braun, J. H. Abeles, and P. J. Delfyett. "Noise in Fundamental and Harmonic Mode-Locked Semiconductor Lasers: Experiments and Simulations." *IEEE J. of Quantum Elect.* **39:**838–849, 2003.

11. J.-C. Diels, Jason Jones, and Ladan Arissian. "Applications to Sensors of Extreme Sensitivity." In Jun Ye and Stephen Cundiff, (eds.) *Femtosecond Optical Frequency Comb: Principle, Operation and Applications,* Springer, New York, 2005, chapter 13, 333–354.
12. F. Aronowitz and R. J. Collins. "Mode Coupling due to Backscattering in a He-Ne Traveling-Wave Ring Laser." *Appl Phys. Lett.* **9:**55–58, 1966.
13. F. Aronowitz. "The Laser Gyro." In Ross, (ed.) *Laser Applications,* Academic Press, New York, 1971, 133–200.
14. J.-C. Diels, I. C. McMichael, J. J. Fontaine, and C. Y. Wang. "Subpicosecond Pulse Shape Measurement and Modeling of Passively Mode locked Dye Lasers Including Saturation and Spatial Hole Burning." In K. B. Eisenthal, R. M. Hochstrasser, W. Kaiser, and A. Laubereau, (eds.) *Picosecond Phenomena III,* Springer-Verlag, New York, 1982, 116–119.
15. M. L. Dennis, J.-C. Diels, and M. Lai. "The Femtosecond Ring Dye Laser: A Potential New Laser Gyro." *Opt. Lett.* **16:**529–531, 1991.
16. Ming Lai, Jean-Claude Diels, and Michael Dennis. "Nonreciprocal Measurements in fs Ring Lasers." *Opt. Lett.* **17:**1535–1537, 1992.
17. Ladan Arissian and Jean-Claude Diels. "Repetition Rate Spectroscopy of the Dark Line Resonance in Rubidium." *Opt. Comm.* **264:**169–173, 2006.
18. Matthew J. Bohn and Jean-Claude Diels. "Bidirectional Kerr-Lens Mode-Locked Femtosecond Ring Laser." *Opt. Comm.* **141:**53–58, 1997.
19. Scott Diddams, Briggs Atherton, and Jean-Claude Diels. "Frequency Locking and Unlocking in a Femtosecond Ring Laser with the Application to Intracavity Phase Measurements." *Appl. Phys. B* **63:**473–480, 1996.
20. Czeslaw Radzewicz, Gary W. Pearson, and Jerzy S. Krasinski. "Use of ZnS as an Additional Highly Nonlinear Intracavity Self-Focusing Element in a Ti:sapphire Self-Modelocked Laser. *Opt. Comm.* **102:**464–468, 1993.
21. M. J. Bohn, R. J. Jones, and J.-C. Diels. "Mutual Kerr-Lens Mode-Locking." *Opt. Comm.* **170:**85–92, 1999.
22. G. P. Agrawal. *Nonlinear Fiber Optics.* Academic Press, Boston, 1995, ISBN 0-12-045142-5.
23. G. E. Stedman, Z. Li, C. H. Rowe, A. D. McGregor, and H. R. Bilger. "Harmonic Analysis in a Large Ring Laser with Backscatter-Induced Pulling." *Physical Review A* **51**(6), June 1995.
24. Matthew J. Bohn, Jean-Claude Diels, and R. K. Jain. "Measuring Intracavity Phase Changes Using Double Pulses in a Linear Cavity." *Opt. Lett.* **22:**642–644, 1997.
25. Ming Lai and Jean-Claude Diels. "Wave-Particle Duality of a Photon in Emission." *J. of the Opt Soc. Am. B* **9:**2290–2294, 1992.
26. D. Gnass, N. P. Ernsting, and F. P. Schaefer. "Sagnac Effect in the Colliding-Pulse-Mode-Locked Dye Ring Laser." *Appl. Phys. B* **B-53:**119–120, 1991.
27. F. Krausz, Ch. Spielman, T. Brabec, E. Wintner, and A. J. Schmidt. "Generation of 33-fs Optical Pulses from a Solid-State Laser," *Opt. Lett.* **17:**204, 1992.
28. C. Spielmann, P. F. Curley, T. Brabec, and F. Krausz. "Ultrabroadband Femtosecond Lasers." *IEEE J. Quant. Elec.* **QE-30:**1100–1114, 1994.
29. A. E. Siegman. "An Antiresonant Ring Interferometer for Coupled Laser Cavities, Laser Output Coupling, Mode-Locking, and Cavity Dumping." *IEEE J. Quantum Electron.* **QE-9:**247–250, 1973.
30. N. Jamasbi, J.-C. Diels, and L. Sarger. "Study of a Linear Femtosecond Laser in Passive and Hybrid Operation." *J. of Modern Optics* **35:**1891–1906, 1988.
31. D. T. Reid, M. Padgett, C. McGowan, W. E. Sleat, and W. Sibbett. "Light-Emitting Diodes as Measurement Devices for Femtosecond Laser Pulses." *Opt. Lett.* **22:**233–235, 1997.
32. E. S. Wachman, D. C. Edelstein, and C. L. Tang. "Continuous-Wave Mode-Locked and Dispersion Compensated fs Optical Parametric Oscillator." *Opt. Lett.* **15:**136–139, 1990.
33. Xianmei Meng, Jean-Claude Diels, Dietrich Kuehlke, Robert Batchko, and Robert Byer. "Bidirectional, Synchronously Pumped, Ring Optical Parametric Oscillator." *Opt. Lett.* **26:**265–267, 2001.
34. Xianmei Meng, Raphael Quintero, and Jean-Claude Diels. "Intracavity Pumped Optical Parametric Bidirectional Ring Laser as a Differential Interferometer." *Opt. Comm.* **233:**167–172, 2004.
35. R. P. Feynman, F. L. Vernon, and R. W. Hellwarth. "Geometrical Representation of the Schroedinger Equation for Solving Maser Problems." *J. Appl. Phys.* **28:**49–52, 1957.
36. Rafael Quintero-Torres, Mark Ackerman, Martha Navarro, and Jean-Claude Diels. "Scatterometer Using a Bidirectional Ring Laser." *Opt. Comm.* **241:**179–183, 2004.

37. M. Navarro, O. Chalus, and Jean-Claude Diels. "Mode-Locked Ring Lasers for Backscattering Measurement of Mirror." *Opt. Lett.* **31:**2864–2866, 2006.

38. R. G. Brewer and R. L. Shoemaker. "Photon Echoes and Optical Nutation in Molecules." *Phys. Rev. Lett.* **27:**631–634, 1971.

39. R. G. Brewer and R. L. Shoemaker. "Optical Free Induction Decay. *Phys. Rev. A* **6:**2001–2007, 1972.

40. P. R. Berman, J. M. Levy, and R. G. Brewer. "Coherent Optical Transient Study of Molecular Collisions: Theory and Observations." *Phys. Rev.* **11:**1668–1688, 1975.

41. N. F. Ramsey. "A Molecular Beam Resonance Method with Separated Oscillating Fields." *Phys. Rev.* **78:**695–699, 1950.

42. M. M. Salour and C. Cohen-Tannoudji. "Observation of Ramsey's Interference Fringes in the Profile of Doppler-Free Two-Photon Resonances." *Phys. Rev. Lett.* **38:**757–760, 1977.